Computational Investigation of Novel Half-Normal Data Using Improved Type-II Adaptive Progressive Censoring and Its Application to the Shasta Reservoir

Ohud A. Alqasem[1], Mazen Nassar[2], Maysaa Elmahi Abd Elwahab[1] and Ahmed Elshahhat[3,*]

[1] Department of Mathematical Sciences, College of Science, Princess Nourah bint Abdulrahman University, P.O. Box 84428, Riyadh, 11671, Saudi Arabia

[2] Department of Statistics, Faculty of Science, King Abdulaziz University, Jeddah, 21589, Saudi Arabia

[3] Faculty of Technology and Development, Zagazig University, Zagazig, 44519, Egypt

INFORMATION

Keywords:
New half-normal
shasta reservoir
improved adaptive progressive
Markovian chain
Bayesian
likelihood and spacings functions

DOI: 10.23967/j.rimni.2025.10.65541

SCIPEDIA
Revista Internacional de Métodos Numéricos para Cálculo y Diseño en Ingeniería
RIMNI

Computational Investigation of Novel Half-Normal Data Using Improved Type-II Adaptive Progressive Censoring and Its Application to the Shasta Reservoir

Ohud A. Alqasem[1], **Mazen Nassar**[2], **Maysaa Elmahi Abd Elwahab**[1] **and Ahmed Elshahhat**[3,*]

[1]Department of Mathematical Sciences, College of Science, Princess Nourah bint Abdulrahman University, P.O. Box 84428, Riyadh, 11671, Saudi Arabia

[2]Department of Statistics, Faculty of Science, King Abdulaziz University, Jeddah, 21589, Saudi Arabia

[3]Faculty of Technology and Development, Zagazig University, Zagazig, 44519, Egypt

ABSTRACT

Shasta Reservoir is the largest in California, formed by Shasta Dam on the Sacramento River, and plays a major role in the Central Valley Project (CVP) by providing water storage, flood control, hydroelectric power, and irrigation. This study employs advanced statistical methods to evaluate the reservoir's reliability and operational risks using censored hydrological data. We propose an improved adaptive progressive censoring plan and apply established statistical techniques, maximum likelihood and maximum product of spacings, alongside Bayesian estimation. The Bayes estimates are obtained through the squared error loss function and based on two sources for the observed data, namely the likelihood and spacing functions. The focus is on estimating the distribution's scale parameter and two critical reliability metrics: the reliability function and the hazard rate function. The approximate confidence intervals based on the two classical approaches of the scale parameter and reliability metrics are studied. The highest posterior density credible intervals are also discussed. A simulation study evaluates the model's accuracy under diverse data scenarios, and its practical utility is demonstrated through real-world data from Shasta Reservoir. The problem of optimizing data collection strategies is discussed with the same real data. The findings underscore the model's value in enhancing reservoir reliability assessments, offering actionable insights for hydrology, disaster preparedness, and sustainable resource management.

OPEN ACCESS

Received: 15/03/2025

Accepted: 12/06/2025

Published: 22/09/2025

DOI
10.23967/j.rimni.2025.10.65541

Keywords:
New half-normal
shasta reservoir
improved adaptive progressive
Markovian chain
Bayesian
likelihood and spacings functions

1 Introduction

Over the past years, there has been a significant emphasis from numerous authors on devising flexible and highly adaptable statistical distributions by implementing a variety of transformation

*Correspondence: Ahmed Elshahhat (aelshahhat@ftd.zu.edu.eg).

approaches. Practically, there are many everyday situations where observations are bound to certain values, like proportions, percentages, and fractions, in which the case of distributions having unbounded support becomes inappropriate. Therefore, Bakouch et al. [1] suggested a novel one-parameter model defined on the unit interval called the unit half normal (UHN) distribution. The random variable Y is said to have the UHN distribution, denoted by $Y \sim \mathrm{UHN}(\sigma)$, where $\sigma > 0$ is a scale parameter, if its respective probability density function (PDF), say $f(\cdot)$, reliability function (RF), say $R(\cdot)$, and hazard rate function (HRF), say $h(\cdot)$, are given by

$$f(y;\sigma) = \frac{2}{\sigma(1-y)^2}\phi\left(\frac{y}{\sigma(1-y)}\right),\ 0 \leqslant y < 1, \tag{1}$$

$$R(y;\sigma) = 2\left[1 - \Phi\left(\frac{y}{\sigma(1-y)}\right)\right] \tag{2}$$

and

$$h(y;\sigma) = \frac{\phi\left(\frac{y}{\sigma(1-y)}\right)}{\sigma(1-y)^2\left[1-\Phi\left(\frac{y}{\sigma(1-y)}\right)\right]}, \tag{3}$$

where $\phi(.)$ and $\Phi(.)$ are the PDF and cumulative distribution function (CDF) of the standard normal distribution, respectively. Taking some options of σ, Fig. 1 indicates that the UHN density (1) takes a decreasing or unimodal shape, while the UHN failure rate (3) is always decreasing. Bakouch et al. [1] also stated that the new UHN model provides better fit in the adjustment of actual data compared to other well-known models in the literature, including beta, unit-Lindley, unit-logistic, and Kumaraswamy distributions. One notable feature of the UHN distribution is that it is a single-parameter model. In the context of complex censoring schemes, using distributions with two or three parameters often results in more complicated inference procedures and increased computational challenges, primarily due to the complexity of their likelihood functions. As a result, the UHN distribution is a strong candidate for use in reliability studies, offering both simplicity and effectiveness.

Due to limited time and financial aid, full-life testing experiments are often impractical in various fields, such as engineering and medical studies. This has resulted in the evolution and widespread use of censored samples, which conclude when a particular portion of units have failed, see [2] for more details. One notable method that has gained traction among experimenters and reliability experts is the progressive Type-II censoring (PT2C) scheme. In this approach, n units are subjected to a life test. Before the test begins, the experimenter employs a progressive censoring plan, denoted as $\mathbf{R} = (R_1, \ldots, R_m)$, to acquire the number m of failed units. After the first failure $Y_{1:m:n}$ occurs, a random sample of R_1 surviving products is drawn from the test. Next, upon the second failure $Y_{2:m:n}$, a random sample of R_2 is extracted from the remaining products. This process continues until all remaining units, represented by R_m, are drawn following the m^{th} failure, which has a lifetime of $Y_{m:m:n}$. Many authors considered this plan; for example, Balakrishnan et al. [3], Rastogi and Tripathi [4], Dey et al. [5], and Anakha and Chacko [6]. Recently, several generalizations of the PT2C scheme have been considered. One such generalization is the adaptive progressive Type-II censoring (APT2C) scheme proposed by Ng et al. [7]. This scheme aims to enhance the efficiency of statistical inference by ensuring that a predetermined number of failures is observed. For additional studies related to the APT2C scheme, one can refer to Ye et al. [8], Hemmati and Khorram [9], Nassar and Abo-Kasem [10], Kumari et al. [11], and Lv et al. [12].

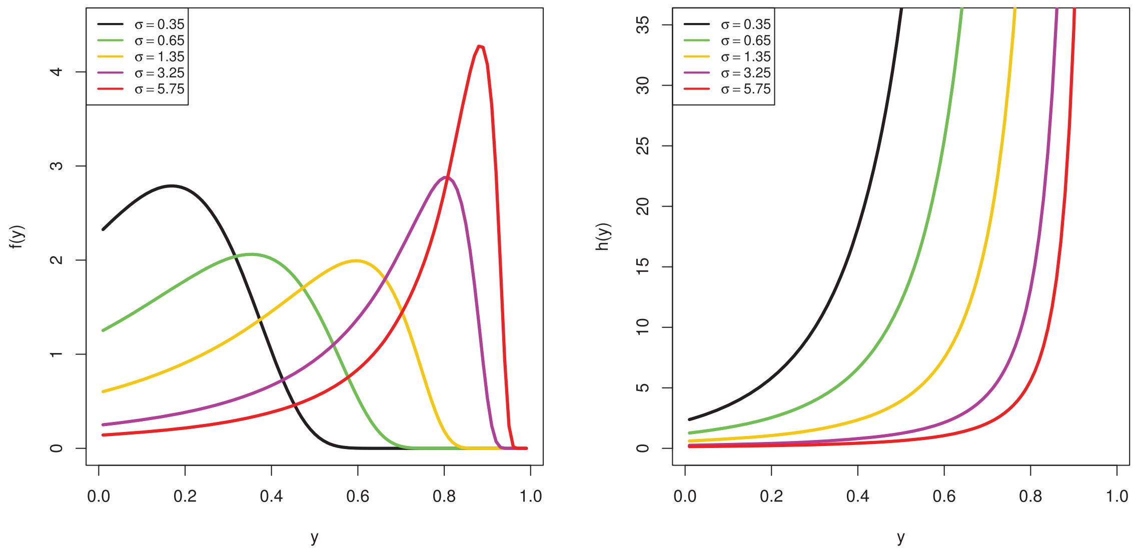

Figure 1: The PDF (left) and HRF (right) shapes of the UHN distribution

Ng et al. [7] found that the APT2C plan is effective for statistical inference when test duration is not a significant factor. However, if the testing time becomes very long, as in the case of trustworthy items, the APT2C strategy fails to guarantee an appropriate total test length. To fix this challenge, Yan et al. [13] presented a new censoring methodology called the improved APT2C (IAPT2C) method. This technique effectively ensures that the experiment is conducted within the established time range. In this strategy, there are n units under the test with a prefixed m number of failures, and a progressive censoring plan $\mathbf{R} = (R_1, \ldots, R_m)$. Furthermore, we have have two time limits, T_1 and T_2, where $T_1 < T_2$. This scheme's design is similar to that of the PT2C, where after observing the i^{th} failure time $Y_{i:m:n}$, R_i units of the surviving objects are randomly eliminated from the test. However, the experiment is halted under one of the following three conditions:

1. If $Y_{m:m:n} < T_1$, the experiment stops at $Y_{m:m:n}$. The acquired sample in this case is the PT2C sample, denoted by $Y_{1:m:n} < \ldots < Y_{m:m:n}$ with progressive censoring plan $(R_1, \ldots, R_m)$, where $R_m = n - m - \sum_{i=1}^{m-1} R_i$. This case is referred to as Case I.
2. If $T_1 < Y_{m:m:n} < T_2$, the test concludes at $Y_{m:m:n}$, given that no items are eliminated beyond the first time limit T_1. After observing the last failure time $Y_{m:m:n}$, the remaining items are removed from the test. This case describes the APT2C sample, denoted by $Y_{1:m:n} < \ldots < Y_{d_1:m:n} < T_1 < Y_{d_1+1:m:n} < \ldots < Y_{m:m:n}$, with progressive censoring plan $(R_1, \ldots, R_{d_1}, 0, \ldots, 0, R_m^*)$, where $R_m^* = n - m - \sum_{i=1}^{d_1} R_i$, where d_1 is the number of observed failures before time limit T_1. This case is referred to as Case II.
3. If $T_1 < T_2 < Y_{m:m:n}$, the experiment is stopped at T_2. Likewise the APT2C sample, no items are removed from the test after observing T_2. In this case, we have the sample $Y_{1:m:n} < \ldots < Y_{d_1:m:n} < T_1 < Y_{d_1+1:m:n} < \ldots < Y_{d_2:m:n} < T_2$, with progressive censoring plan $(R_1, \ldots, R_{d_1}, 0, \ldots, 0, R^\star)$, where $R^\star = n - d_2 - \sum_{i=1}^{d_1} R_i$, where d_2 is the number of observed failures before time limit T_2. This case is referred to as Case III.

Fig. 2 presents the schematic visualization of the IAPT2C plan. Let $y_i = y_{i:m:n}$ is the realization of $Y_i = Y_{i:m:n}, i = 1, \ldots, m$. Then, based on the gathered observed IAPT2C sample $\underline{\mathbf{y}} = (y_1 < \ldots < y_{d_1} < T_1 < \ldots < y_{d_2} < T_2)$, with removal pattern $\mathbf{R} = (R_1, \ldots, R_{d_1}, 0, \ldots, 0, R^*)$. Then, the likelihood function (LF) of the observed data can be expressed, without a constant term, as

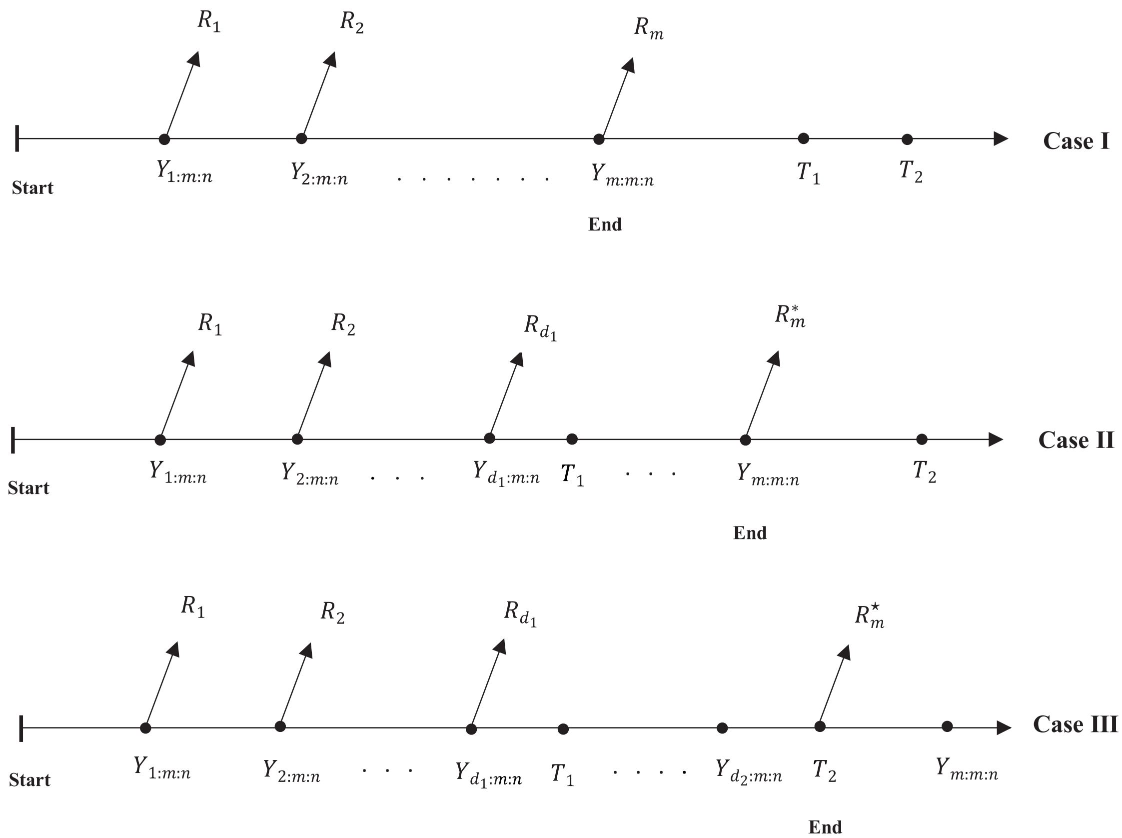

Figure 2: Schematic representation of the IAPT2C plan

$$L(\sigma|\underline{\mathbf{y}}) = \prod_{i=1}^{D_2} f(y_i;\sigma) \prod_{i=1}^{D_1} [1 - F(y_i;\sigma)]^{R_i} [1 - F(\tau;\sigma)]^{R^*}, \tag{4}$$

where $F(y_i;\sigma) = 1 - R(y_i;\sigma)$, D_1, D_2, τ and R^* are given by

$$D_1 = \begin{cases} m, \text{ for Case-I} \\ d_1, \text{ for Case-II} \\ d_1, \text{ for Case-III} \end{cases}, D_2 = \begin{cases} m, \text{ for Case-I} \\ m, \text{ for Case-II} \\ d_2, \text{ for Case-III} \end{cases},$$

and

$$\tau = \begin{cases} 0, \text{ for Case-I} \\ y_m, \text{ for Case-II} \\ T_2, \text{ for Case-III} \end{cases}, R^* = \begin{cases} 0, \text{ for Case-I} \\ n - m - \sum_{i=1}^{d_1} R_i, \text{ for Case-II} \\ n - d_2 - \sum_{i=1}^{d_1} R_i, \text{ for Case-III} \end{cases}.$$

In the past two years, several studies have examined both classical and Bayesian estimation methods for certain lifetime distributions using IAPT2C data. For more details, refer to Asadi et al. [14], Dutta and Kayal [15], Alam and Nassar [16], Zhang and Yan [17], and Alotaibi et al. [18]. From a classical estimation perspective, this study examines another estimation method known as the maximum product of spacings (MPS) estimation method. This approach, presented by Cheng and Amin [19] and Ranneby [20] independently, serves as an alternative to the maximum likelihood method. The MPS estimators (MPSEs) share desirable properties with maximum likelihood estimators (MLEs) and can sometimes outperform them, particularly in cases of small sample sizes and heavy-tailed distributions, see [21] for more details. Like the MLEs, the MPSEs possess the invariance property, allowing us to estimate any function of the unknown parameters by simply substituting the true parameter values with the obtained MPSEs. Using the IAPT2C sample, the MPSE of the unknown parameter σ can be obtained by maximizing the following spacings function (SF), without a constant term, concerning σ

$$S(\sigma|\underline{\mathbf{y}}) = \prod_{i=1}^{D_2+1} \Delta_i \prod_{i=1}^{D_1} [1 - F(y_i;\sigma)]^{R_i} [1 - F(\tau;\sigma)]^{R^*}, \tag{5}$$

where $\Delta_i = F(y_i;\sigma) - F(y_{i-1};\sigma)$. Many studies have utilized the MPS estimation method. For example, see Innocent et al. [22], Alsadat et al. [23], Abonongo and Abonongo [24], and Dutta et al. [25].

We are motivated to conduct this study for several reasons: (1) The UHN distribution provides practical flexibility and has shown better performance than nine other distributions, with one or two parameters, when applied to real-world data, as demonstrated later in the data analysis section. This makes it a promising option for conducting reliability analysis in systems like the Shasta Reservoir. Given the notable flexibility of the UHN distribution in analyzing bounded real-world data compared to existing models, this study represents, to the best of our knowledge, the first work to investigate its reliability estimation, particularly in the context of censoring schemes. (2) The IAPT2C plan addresses the shortcomings of traditional APT2C schemes in reliability studies. It enhances the accuracy and efficiency of statistical inference, particularly when assessing highly reliable products. (3) Exploring the use of different data sources in Bayesian estimation, specifically comparing Bayes estimates based on the LF and SF, enhances the methodological flexibility and strengthens the statistical analysis. (4) Few studies have addressed the challenge of determining the optimal progressive censoring scheme for the IAPT2C plan, which aims to balance data collection efficiency and statistical accuracy. Before proceeding, and for distinction, Fig. 3 shows a flowchart of all the estimation methodologies proposed in this work. Accordingly, we can list the objectives of the study as follows:

- Derive point estimates, MLE and MPSEs, and approximate confidence intervals (ACIs) for the UHN distribution's scale parameter σ, RF, and HRF.
- Develop Bayesian estimates under the squared error loss function using LF-based observed data and SF-based observed data. The Markov Chain Monte Carlo (MCMC) sampling method is implemented to compute the estimates and construct highest posterior density (HPD) credible intervals.
- Conduct a simulation experiment to compare the performance of classical and Bayesian methods, evaluate the coverage percentages and interval widths of ACIs and HPD intervals.
- Analyze real-world data from the Shasta Reservoir to showcase the applicability of the proposed methods and the UHN model's superior fit over nine competing distributions.
- Explore criteria for selecting the optimal progressive censoring scheme under the IAPT2C plan.

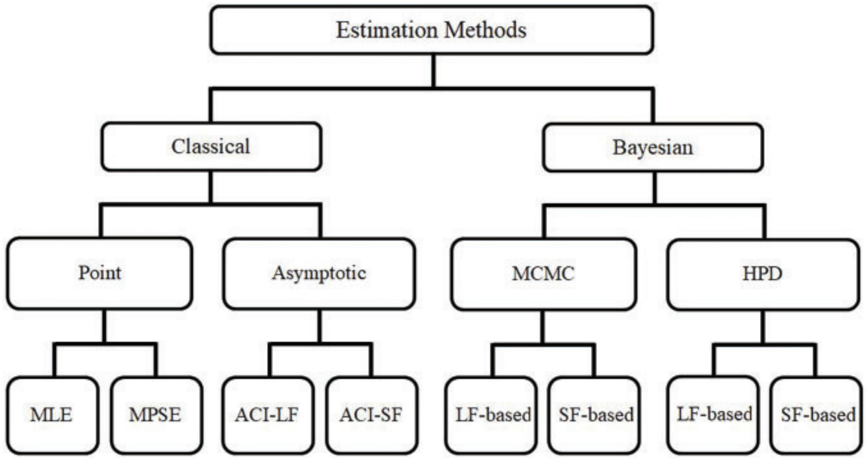

Figure 3: Flowchart of the proposed estimation approaches

The rest of this paper is structured as follows: Section 2 shows the MLEs as well as the ACIs for the unknown parameter σ, RF, and HRF. The MPSEs and the associated ACIs are discussed in Section 3. The Bayes estimates using both LF and SF are investigated in Section 4. The simulation design as well as the numerical outcomes are presented in Section 5. One real data set is examined in Section 6. Section 7 presents some criteria to select the optimal progressive censoring plan. The paper is concluded in Section 8.

2 Likelihood Estimation

In this section, the MLEs and ACIs of σ, RF, and HRF of the UHN distribution are discussed in the presence of IAPT2C data. Let $\underline{\mathbf{y}} = (y_1 < \ldots < y_{d_1} < T_1 < \ldots < y_{d_2} < T_2)$, be an IAPT2C sample from the UHN distribution with removal pattern $\mathbf{R} = (R_1, \ldots, R_{d_1}, 0, \ldots, 0, R^*)$. Then, the LF can be written using (1), (2), and (4), after ignoring constant term, as

$$L(\sigma|\underline{\mathbf{y}}) = \frac{1}{\sigma^{D_2}} \prod_{i=1}^{D_2} e^{-\frac{x_i^2}{2\sigma^2}} \prod_{i=1}^{D_1} \left[1 - \Phi\left(\frac{x_i}{\sigma}\right)\right]^{R_i} \left[1 - \Phi\left(\frac{\eta}{\sigma}\right)\right]^{R^*}, \tag{6}$$

where $x_i = y_i/(1 - y_i)$ and $\eta = \tau/(1 - \tau)$. The log-LF of (6) follows

$$l(\sigma|\underline{\mathbf{y}}) = -D_2 \log(\sigma) - \frac{1}{2\sigma^2} \sum_{i=1}^{D_2} x_i^2 + \sum_{i=1}^{D_1} R_i \log\left[1 - \Phi\left(\frac{x_i}{\sigma}\right)\right] + R^* \log\left[1 - \Phi\left(\frac{\eta}{\sigma}\right)\right]. \tag{7}$$

There are two methods to obtain the MLE of the unknown parameter σ. The first method involves maximizing the objective function in (7) concerning σ, which can be accomplished using any numerical method. The second method involves solving the following normal equation

$$\frac{dl(\sigma|\underline{\mathbf{y}})}{d\sigma} = -\frac{D_2}{\sigma} + \frac{1}{2\sigma^3} \sum_{i=1}^{D_2} x_i^2 + \sum_{i=1}^{D_1} \frac{R_i \varphi(x_i;\sigma)}{1 - \Phi\left(\frac{x_i}{\sigma}\right)} + \frac{R^* \varphi(\eta;\sigma)}{1 - \Phi\left(\frac{\eta}{\sigma}\right)} = 0, \tag{8}$$

where $\varphi(x_i;\sigma) = \frac{x_i \phi\left(\frac{x_i}{\sigma}\right)}{\sigma^2}$. One can see that the MLE of σ cannot be acquired explicitly. We use the Newton-Raphson iteration technique to calculate the MLE of σ, represented by $\hat{\sigma}$. Then, using the invariance property of the MLE, we can obtain the MLEs of RF and HRF at time t, respectively, as

$$\hat{R}(t) = 2\left[1 - \Phi\left(\frac{t^*}{\hat{\sigma}}\right)\right]$$

and

$$\hat{h}(t) = \frac{\phi\left(\frac{t^*}{\hat{\sigma}}\right)}{\hat{\sigma}(1-t)^2\left[1 - \Phi\left(\frac{t^*}{\hat{\sigma}}\right)\right]},$$

where $t^* = t/(1-t)$.

The asymptotic normality of MLEs is a significant result in statistical theory. It enables us to construct ACIs for both the parameters of interest and any functions of these parameters. Using this approach and under some mild regularity conditions, it is known that $\hat{\sigma} \sim N(\sigma, var(\hat{\sigma}))$, where $var(\hat{\sigma})$ refers to the variance of the MLE $\hat{\sigma}$. In our analysis, we estimate this variance through inverting the negative of second-order derivative of (7) as

$$\widehat{var}(\hat{\sigma}) = \left[-\frac{d^2 l(\sigma|\underline{\mathbf{y}})}{d\sigma^2}\right]^{-1}_{\sigma=\hat{\sigma}},$$

with

$$\frac{d^2 l(\sigma|\underline{\mathbf{y}})}{d^2\sigma} = \frac{D_2}{\sigma^2} - \frac{3}{2\sigma^4}\sum_{i=1}^{D_2} x_i^2 + \sum_{i=1}^{D_1} R_i \psi(x_i;\sigma) + R^* \psi(\eta;\sigma),$$

where

$$\psi(x_i;\sigma) = \frac{\varphi(x_i;\sigma)}{\sigma\left[1 - \Phi\left(\frac{x_i}{\sigma}\right)\right]}\left\{\frac{x_i^2}{\sigma^2} - \frac{x_i\phi\left(\frac{x_i}{\sigma}\right)}{\sigma\left[1 - \Phi\left(\frac{x_i}{\sigma}\right)\right]} - 2\right\}.$$

Thus, the $100(1-\alpha)\%$ ACI of the unknown parameter σ is

$$\left[\hat{\sigma} - z_{\alpha/2}\sqrt{\widehat{var}(\hat{\sigma})}, \hat{\sigma} + z_{\alpha/2}\sqrt{\widehat{var}(\hat{\sigma})}\right],$$

where $z_{\alpha/2}$ is derived from the standard normal distribution. On the other hand, we need to get the variances of $\hat{R}(t)$ and $\hat{h}(t)$ to construct the ACIs for the RF and HRF. In this work, we employ the delta method to get approximate estimates for these variances. Applying this method, we can get the approximate estimated variances of $\hat{R}(t)$ and $\hat{h}(t)$, respectively, as

$$\widehat{var}(\hat{R}) \approx \hat{R}_\sigma \widehat{var}(\hat{\sigma})\hat{R}_\sigma^\top \text{ and } \widehat{var}(\hat{h}) \approx \hat{h}_\sigma \widehat{var}(\hat{\sigma})\hat{h}_\sigma^\top,$$

where $\hat{R} \equiv \hat{R}(t)$, $\hat{h} \equiv \hat{h}(t)$, and

$$\hat{R}_\sigma = 2\varphi(t;\hat{\sigma}) \text{ and } \hat{h}_\sigma = \frac{\phi\left(\frac{t^*}{\hat{\sigma}}\right)}{\hat{\sigma}^2(t-1)^2\left[1 - \Phi\left(\frac{t^*}{\hat{\sigma}}\right)\right]}\left\{\frac{t^*}{\hat{\sigma}^2} - \frac{\hat{\sigma}t^*\varphi(x_i;\hat{\sigma})}{\left[1 - \Phi\left(\frac{t^*}{\hat{\sigma}}\right)\right]} - 1\right\}. \tag{9}$$

Then, the $100(1-\alpha)\%$ ACIs of RF and HRF are

$$\left[\hat{R} - z_{\alpha/2}\sqrt{\widehat{var}(\hat{R})}, \hat{R} + z_{\alpha/2}\sqrt{\widehat{var}(\hat{R})}\right] \text{ and } \left[\hat{h} - z_{\alpha/2}\sqrt{\widehat{var}(\hat{h})}, \hat{h} + z_{\alpha/2}\sqrt{\widehat{var}(\hat{h})}\right].$$

3 Spacings Estimation

This section studies the MPSEs and ACIs of σ, RF, and HRF of the UHN distribution based on IAPT2C data. Using an IAPT2C sample sample $\underline{\mathbf{y}} = (y_1 < \ldots < y_{d_1} < T_1 < \ldots < y_{d_2} < T_2)$ from the UHN distribution, we can write the spacings $\bar{\Delta}_i = F(y_i;\sigma) - F(y_{i-1};\sigma)$ as follows:

$$\Delta_i = 2\left[\Phi\left(\frac{x_i}{\sigma}\right) - \Phi\left(\frac{x_{i-1}}{\sigma}\right)\right], i = 1,\ldots,d_2. \tag{10}$$

Thus, using (2), (5), and (10), the SF can be expressed, without constant term, as given below:

$$S(\sigma|\underline{\mathbf{y}}) = \prod_{i=1}^{D_2+1}\Delta_i\prod_{i=1}^{D_1}\left[1-\Phi\left(\frac{x_i}{\sigma}\right)\right]^{R_i}\left[1-\Phi\left(\frac{\eta}{\sigma}\right)\right]^{R^*}. \tag{11}$$

The natural logarithm of (11), denoted by $s(\sigma|\underline{\mathbf{y}}) = \log[S(\sigma|\underline{\mathbf{y}})]$, follow

$$s(\sigma|\underline{\mathbf{y}}) = \sum_{i=1}^{D_2+1}\log(\Delta_i) + \sum_{i=1}^{D_1}R_i\log\left[1-\Phi\left(\frac{x_i}{\sigma}\right)\right] + R^*\log\left[1-\Phi\left(\frac{\eta}{\sigma}\right)\right]. \tag{12}$$

The MPSE of σ, denoted by $\tilde{\sigma}$, can be obtained through maximizing (12), or by solving the following normal equation

$$\frac{ds(\sigma|\underline{\mathbf{y}})}{d\sigma} = 2\sum_{i=1}^{D_2+1}\frac{\varphi(x_{i-1};\sigma)-\varphi(x_i;\sigma)}{\Delta_i} + \sum_{i=1}^{D_1}\frac{R_i\varphi(x_i;\sigma)}{1-\Phi\left(\frac{x_i}{\sigma}\right)} + \frac{R^*\varphi(\eta;\sigma)}{1-\Phi\left(\frac{\eta}{\sigma}\right)} = 0. \tag{13}$$

As with the case of obtaining the MLE of σ, the MPSE $\tilde{\sigma}$ cannot be derived explicitly. To calculate the MPSE $\tilde{\sigma}$, we employ the Newton-Raphson iteration technique. Subsequently, by using the invariance property of the MPSE, we can determine the MPSEs for the RF and HRF at time t, as

$$\tilde{R}(t) = 2\left[1-\Phi\left(\frac{t^*}{\tilde{\sigma}}\right)\right]$$

and

$$\tilde{h}(t) = \frac{\phi\left(\frac{t^*}{\tilde{\sigma}}\right)}{\tilde{\sigma}(1-t)^2\left[1-\Phi\left(\frac{t^*}{\tilde{\sigma}}\right)\right]}.$$

By utilizing the asymptotic normality of the MPSE, we can construct ACIs for both the parameter σ of interest and the two reliability metrics. This approach reveals that $\tilde{\sigma} \sim N(\sigma, var(\tilde{\sigma}))$, where $var(\tilde{\sigma})$ denotes the variance of the MPSE $\tilde{\sigma}$. In our analysis, we estimate the variance of the MPSE $\tilde{\sigma}$ as follows:

$$\widetilde{var}(\tilde{\sigma}) = \left[-\frac{d^2s(\sigma|\underline{\mathbf{y}})}{d\sigma^2}\right]^{-1}_{\sigma=\tilde{\sigma}},$$

where

$$\frac{d^2 s(\sigma|\underline{\mathbf{y}})}{d^2\sigma} = 2\sum_{i=1}^{D_2+1}\frac{\acute{\varphi}(x_{i-1};\sigma)-\acute{\varphi}(x_i;\sigma)}{\Delta_i} - 2\sum_{i=1}^{D_2+1}\frac{[\varphi(x_{i-1};\sigma)-\varphi(x_i;\sigma)]^2}{\Delta_i^2} + \sum_{i=1}^{D_1} R_i\psi(x_i;\sigma) + R^*\psi(\eta;\sigma),$$

where

$$\acute{\varphi}(x_i;\sigma) = \frac{x_i\phi\left(\frac{x_i}{\sigma}\right)}{\sigma^3}\left(2-\frac{x_i^2}{\sigma^2}\right).$$

Thus, the $100(1-\alpha)\%$ ACI of the unknown parameter σ based on the MPSE $\tilde{\sigma}$ can be obtained as $\left[\tilde{\sigma} - z_{\alpha/2}\sqrt{\widetilde{var}(\tilde{\sigma})}, \tilde{\sigma} + z_{\alpha/2}\sqrt{\widetilde{var}(\tilde{\sigma})}\right]$.

For the ACIs of the RF and HRF, we employ the same approach as in the previous section by obtaining the approximate estimates of the variances of the MPSEs $\tilde{R} \equiv \tilde{R}(t)$ and $\tilde{h} \equiv \tilde{h}(t)$ using the delta method. Thus,

$$\widetilde{var}(\tilde{R}) \approx \tilde{R}_\sigma \widetilde{var}(\hat{\sigma})\tilde{R}_\sigma^\top \text{ and } \widetilde{var}(\tilde{h}) \approx \tilde{h}_\sigma \widetilde{var}(\hat{\sigma})\tilde{h}_\sigma^\top,$$

where $\tilde{R}_\sigma$ and $\tilde{h}_\sigma$ are obtained in a manner similar to (9) at the MPSE $\tilde{\sigma}$ instead of $\hat{\sigma}$. Then, the 100 $(1-\alpha)\%$ ACIs of RF and HRF using the MPSE can be obtained, respectively, as

$$\left[\tilde{R} - z_{\alpha/2}\sqrt{\widetilde{var}(\tilde{R})}, \tilde{R} + z_{\alpha/2}\sqrt{\widetilde{var}(\tilde{R})}\right] \text{ and } \left[\tilde{h} - z_{\alpha/2}\sqrt{\widetilde{var}(\tilde{h})}, \tilde{h} + z_{\alpha/2}\sqrt{\widetilde{var}(\tilde{h})}\right].$$

4 Bayesian Estimation

Due to the use of censoring, the resulting sample sizes are often small. In addition, when testing highly reliable units, experiments are often terminated early to save time or resources, resulting in a small sample size. In such cases, classical estimation methods may not perform well and can produce biased or inaccurate estimates. Moreover, the ACIs rely on large-sample approximations, which tend to be unreliable when the sample size is small. The Bayesian estimation approach addresses these limitations by combining prior knowledge about the unknown parameters with the observed data, leading to a posterior distribution that allows for more stable and accurate inference. In this section, the unknown parameter σ and the two reliability measures are estimated using the Bayesian estimation technique. Additionally, we discuss the HPD credible intervals, alongside the Bayesian point estimates for the aforementioned parameters. The two versions of the posterior distribution, the first derived from the LF and the second from the SF, are employed to obtain these Bayesian point and interval estimates. Since no conjugate prior distribution is available for the parameter σ, we utilize the advantageous properties of the gamma distribution and employ it as a prior distribution for σ. The gamma prior is chosen for the parameter σ due to its flexibility in representing a wide range of prior beliefs through adjustable shape and rate parameters. It naturally accommodates the positive support of the unknown parameter. Additionally, the gamma prior simplifies the specification of hyper-parameters through closed-form expressions for moments, facilitating systematic uncertainty quantification. By offering a balance between computational feasibility and theoretical soundness, it provides a practical alternative in the absence of conjugate priors. This choice supports both efficient computation and clear interpretation in posterior inference, making it well-suited for reliable Bayesian estimation. The prior distribution, in this case, can be expressed as

$$p(\sigma) \propto \sigma^{a-1} e^{-b\sigma}, \sigma > 0, a, b > 0. \tag{14}$$

Then, based on the LF in (6) and the SF in (11), the two forms of the posterior distribution can be expressed, respectively, as

$$Q_1(\sigma|\underline{\mathbf{y}}) = \frac{1}{A_1 \sigma^{D_2 - a + 1}} \prod_{i=1}^{D_2} e^{-\frac{x_i^2}{2\sigma^2} - b\sigma} \prod_{i=1}^{D_1} \left[1 - \Phi\left(\frac{x_i}{\sigma}\right)\right]^{R_i} \left[1 - \Phi\left(\frac{\eta}{\sigma}\right)\right]^{R^*} \tag{15}$$

and

$$Q_2(\sigma|\underline{\mathbf{y}}) = \frac{\sigma^{a-1} e^{-b\sigma}}{A_2} \prod_{i=1}^{D_2+1} \Delta_i \prod_{i=1}^{D_1} \left[1 - \Phi\left(\frac{x_i}{\sigma}\right)\right]^{R_i} \left[1 - \Phi\left(\frac{\eta}{\sigma}\right)\right]^{R^*}, \tag{16}$$

where $A_1 = \int_0^\infty p(\sigma) L(\sigma|\underline{\mathbf{y}}) d\sigma$ and $A_2 = \int_0^\infty p(\sigma) S(\sigma|\underline{\mathbf{y}}) d\sigma$. Let $\varpi(\sigma)$ be any function of the unknown parameter σ. Then, based on the squared error loss function, the Bayes estimator using (15), denoted by $\hat{\varpi}^*(\sigma)$, can be obtained as

$$\hat{\varpi}^*(\sigma) = \int_0^\infty \varpi(\sigma) Q_1(\sigma|\underline{\mathbf{y}}) d\sigma. \tag{17}$$

Similarly, the Bayes estimator using (16), denoted by $\tilde{\varpi}^*(\sigma)$, can be derived as

$$\tilde{\varpi}^*(\sigma) = \int_0^\infty \varpi(\sigma) Q_2(\sigma|\underline{\mathbf{y}}) d\sigma. \tag{18}$$

It is evident from (17) and (18) that the Bayes estimators cannot be obtained explicitly because of the complex nature of the posterior distribution. To address this issue, we utilize the MCMC sampling procedure to draw samples from (15) and (16). These samples are then used to compute the Bayes estimates $\hat{\varpi}^*(\sigma)$ and $\tilde{\varpi}^*(\sigma)$. To generate such samples, it is essential to first identify the distributions to which the posterior distributions in equations (15) and (16) correspond. This step is crucial when employing the MCMC procedure, as it informs the selection of the appropriate algorithm. The distributions in (15) and (16) are unknown and cannot be reduced to any known distributions. Thus, we consider using the Metropolis-Hastings (MH) algorithm with a normal proposal distribution to generate the MCMC samples. The steps necessary to generate the MCMC samples utilizing the MH algorithm from the posterior distribution presented in (15) are enumerated below:

Step 1. Set $j = 1$ and $\sigma^{(0)} = \hat{\sigma}$ as initial value.

Step 2. Generate a new value for σ, denoted by $\sigma^{(j)}$, from $Q_1(\sigma|\underline{\mathbf{y}})$ using the MH algorithm.

Step 3. Use $\sigma^{(j)}$ to calculate $R^{(j)}$, $h^{(j)}$.

Step 4. Put $j = j + 1$.

Step 5. Redo steps 2 to 4, M times to get the sequence $\left\{\sigma^{(j)}, R^{(j)}, h^{(j)}\right\}, j = 1, \ldots, M$.

Upon obtaining the MCMC sample, we can obtain the Bayes-LF-based estimates of the unknown parameter σ, RF and HRF, after discarding the first H samples as a burn-in period, respectively, as

$$\hat{\sigma}^* = \frac{1}{M-H}\sum_{j=H+1}^{M}\sigma^{(j)},\ \ \hat{R}^* = \frac{1}{M-H}\sum_{j=H+1}^{M}R^{(j)}\ \text{ and, }\ \hat{h}^* = \frac{1}{M-H}\sum_{j=H+1}^{M}h^{(j)}.$$

On the other hand, to get the HPD credible intervals of the unknown parameter σ, RF and HRF, we first sort the MCMC sample as $\left\{\sigma^{(H+1)} < \ldots < \sigma^{(M)}\right\}$, $\left\{R^{(H+1)} < \ldots < R^{(M)}\right\}$, and $\left\{h^{(H+1)} < \ldots < h^{(M)}\right\}$. Then, the $100(1-\alpha)\%$ HPD interval for σ, for example, follows

$$\left\{\sigma^{(j^*)}, \sigma^{(j^*+(1-\alpha)(M-H))}\right\},$$

where $j^* = B+1, \ldots, M$ is specified such that

$$\sigma^{(j^*+[(1-\alpha)(M-H)])} - \sigma^{(j^*)} = \min_{1\leqslant j\leqslant \alpha(M-H)}\left\{\sigma^{(j+[(1-\alpha)(M-H)])} - \sigma^{(j)}\right\},$$

where $[j]$ refers to the highest integer that does not exceed j.

Likewise, one can use the MH algorithm steps to generate samples from the posterior distribution in $Q_2(\sigma|\mathbf{y})$ (16) employing the MPSE of the unknown parameter σ as the starting value. Then, we can obtain the Bayes estimates of the unknown parameter σ, RF, and HRF as well as the associated HPD credible intervals as in the case of the Bayes-LF-based estimates.

5 Numerical Evaluations

This section uses Monte-Carlo simulations to assess the effectiveness of the offered estimations of σ, $R(t)$, and $h(t)$ developed in the previous sections.

5.1 Simulation Scenarios

To examine how the acquired estimators of σ, $R(t)$, and $h(t)$ work from UHN(1.5) and UHN(2.5), we produce 1,000 samples. At $t = 0.1$, the actual values of $(R(t), h(t))$ are taken as (0.94095, 0.69599) and (0.96455, 0.40809) for UHN(1.5) and UHN(2.5), respectively. To see if the proposed estimators work well in different circumstances, we can look at different combinations of threshold times T_i, $i = 1, 2$, full sample size n, full failure size m, and progressive pattern $\mathbf{R}$. In our scenarios, we have taken $n(= 50, 80)$, m is specified as failure percentage (FP) $\frac{m}{n}(= 50, 80)\%$, and three designs of $\mathbf{R}$, namely: Scheme-1: left censoring, Scheme-2: middle censoring, and Scheme-3: right censoring. Also, the thresholds (T_1, T_2) are utilized as:

- (0.2, 0.3) and (0.4, 0.6) for UHN(1.5);
- (0.3, 0.4) and (0.5, 0.7) for UHN(2.5).

To get an IAPT2C sample, after specifying the values of (n, m), T_i, $i = 1, 2$, and R_i, $i = 1, 2, \ldots, m$, follow the next procedure:

Step 1. Fix the actual value of σ.

Step 2. Get a PT2C sample as:

a. Get an uniform sample (of size m), say $(w_1, w_2, \ldots, w_m)$.

b. Set $\tau_i = w_i^{\left(i+\sum_{j=m-i+1}^{m} R_j\right)^{-1}}$, $i = 1, 2, \ldots, m$.

c. Set $U_i = 1 - \tau_m \tau_{m-1} \cdots \tau_{m-i+1}$ for $i = 1, 2, \ldots, m$.

d. Get a PT2C sample as $Y_i = \dfrac{\sigma \Phi^{-1}(0.5(u_i + 1))}{1 + \sigma \Phi^{-1}(0.5(u_i + 1))}$, $i = 1, 2, \ldots, m$.

Step 3. Find d_1 at T_1, and ignore Y_i, $i = d_1 + d_1 + 2, \ldots, m$.

Step 4. Find the first $m - d_1 - 1$ order statistics (say $Y_{d_1+2}, \ldots, Y_m$) from a truncated distribution $f(y)\left[R\left(y_{d_1+1}\right)\right]^{-1}$ with sample size $n - d_1 - 1 - \sum_{i=1}^{d_1} R_i$.

Step 5. Find the IAPT2C type as:

a. Case-1: If $Y_m < T_1 < T_2$; stop the test at Y_m.

b. Case-2: If $T_1 < Y_m < T_2$; stop the test at Y_m.

c. Case-3: If $T_1 < T_2 < Y_m$; stop the test at T_2.

Once 1000 IAPT2C samples are produced using R 4.2.2 programming software, using the 'maxLik' package (by Henningsen and Toomet [26]), the frequentist estimates as well as their 95% ACI estimates of σ, $R(t)$, or $h(t)$ are evaluated. To obtain the Bayes MCMC and HPD interval estimators of σ, $R(t)$, and $h(t)$, following the M–H steps, we eliminate the first 2000 (out of 12,000) iterations as a "burn-in" period for each unknown parameter. After that, using the 'coda' package (by Plummer et al. [27]), we calculate the MCMC and 95% HPD interval estimates of σ, $R(t)$, or $h(t)$. For clarification, to run these packages, the initial guess of σ is taken to be its actual values suggested before. We also assign the values of (a, b), following the past samples algorithm discussed in Nassar and Elshahhat [28], as:

- (99.99431, 0.014944) and (102.2918, 0.015115) for the Bayes-LF and Bayes-SF, respectively, when UHN(1.5);
- (99.99447, 0.024907) and (102.2918, 0.025192) for the Bayes-LF and Bayes-SF, respectively, when UHN(2.5).

Sensitivity analysis of posterior distributions to prior choices aims to assess how much Bayesian inference (posterior mean, standard deviation, and credible intervals) depends on the selected prior, especially under complex conditions such as those involving censored data. Using the collected 1000 IAPT2C samples (from UHN(1.5) when $(n, m) = (50, 25)$, $(T_1, T_2) = (0.2, 0.3)$, and $R_i = 1$, $i = 1, 2, \ldots, m$), we examine the sensitivity analysis of the posterior distributions from LF-based and SF-based using four different prior choices, including informative, improper, overdispersed, and weak; see Fig. 4. It indicates, from posterior density via LF-based (or SF-based), that the gamma PDF with parameters (a, b) in informative prior (current values assigned before) yields tight, stable posteriors centered near the prior mean, while improper (say, $Uniform(0.1, 10)$), weak (say, $Gamma(1.5, 1)$), and overdispersed (say, $Gamma(3, 2)$) priors allow the data to have more influence, resulting in wider intervals and greater posterior variance, while overdispersed priors show the highest spread and bias. This underscores that posterior inference is sensitive to prior assumptions, particularly when sample size or censoring limits the information from data. As a result, the sensitivity analysis (shown in Fig. 4) examines how robust the backward iterations are over plausible prior configurations.

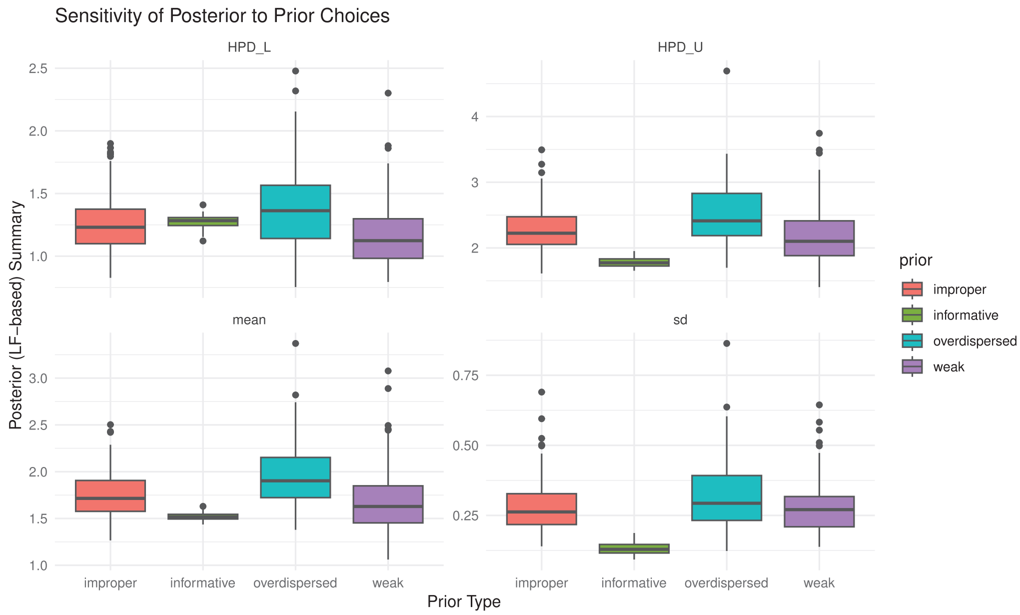

(a) Posterior (LF-based)

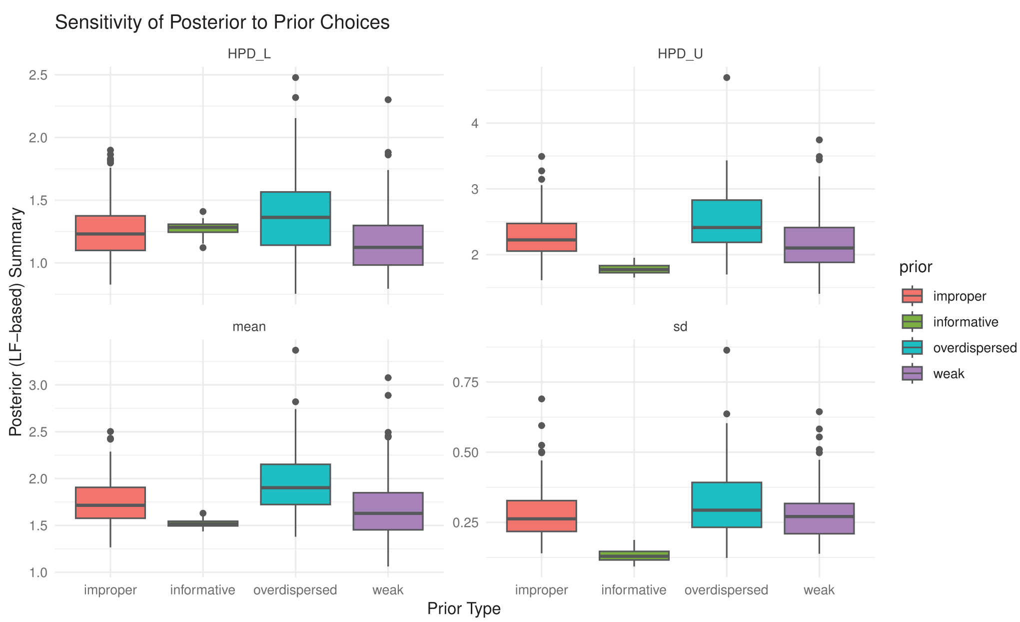

(b) Posterior (SF-based)

Figure 4: Sensitivity of posterior estimates to several prior distributions of σ

To see the convergence of the generated Markovian draws developed from the Bayes-LF (or Bayes-SF) approach of σ, $R(t)$, or $h(t)$, the trace and autocorrelation function (ACF) are plotted; see Fig. 5. It indicates that the level of latency in each chain and the ACF of σ, $R(t)$, or $h(t)$ have a significant connection. This implies that the simulated chains are substantially mixed. It also demonstrates that the Markov chain draws of σ, $R(t)$, or $h(t)$ are well mixed, and so the derived estimations are acceptable. Fig. 6 shows the Brooks-Gelman-Rubin (BGR) diagnostic. It shows that the simulated chains are not significantly different. This proves that the burn-in sample is large enough to ignore the starting point values. Additionally, in Fig. 7, the trace plots using thinning-based (e.g., we took each 5th point) for both Bayes-LF and Bayes-SF approaches are provided. All acquired Markovian chains in Fig. 7 seem to be investigating the same area for the actual parameter value of σ, which is a significant indication. All plots shown in Figs. 5–7 have been created when $\sigma = 1.5$, $(T_1, T_2) = (0.2, 0.3)$, and n[FP%] = 50[50%], **R** is uniformly. As a result, the Bayes estimates using LF-based (or SF-based) of σ, $R(t)$, or $h(t)$ are reliable and acceptable.

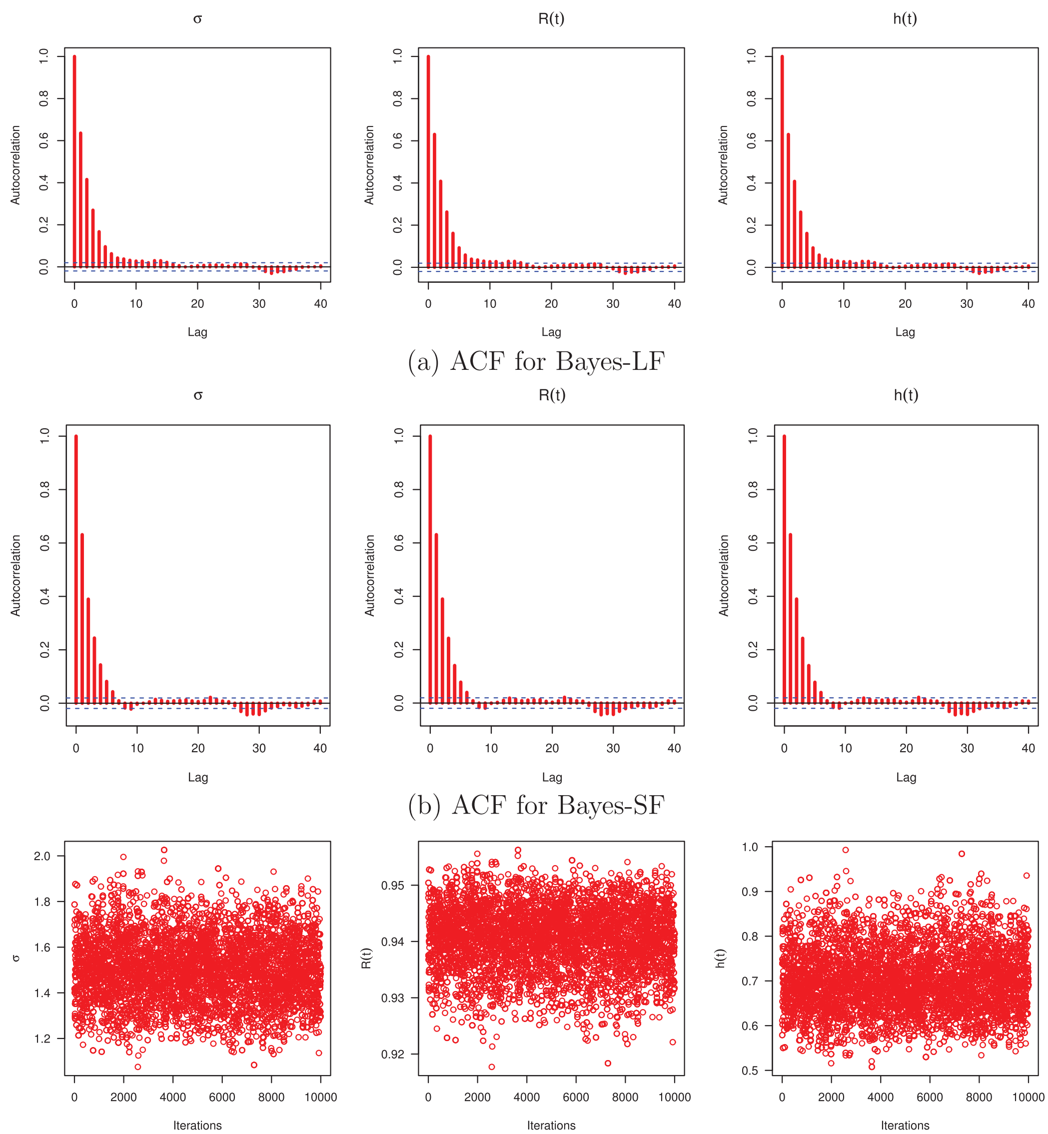

(a) ACF for Bayes-LF

(b) ACF for Bayes-SF

(c) Trace for Bayes-LF

Figure 5: (Continued)

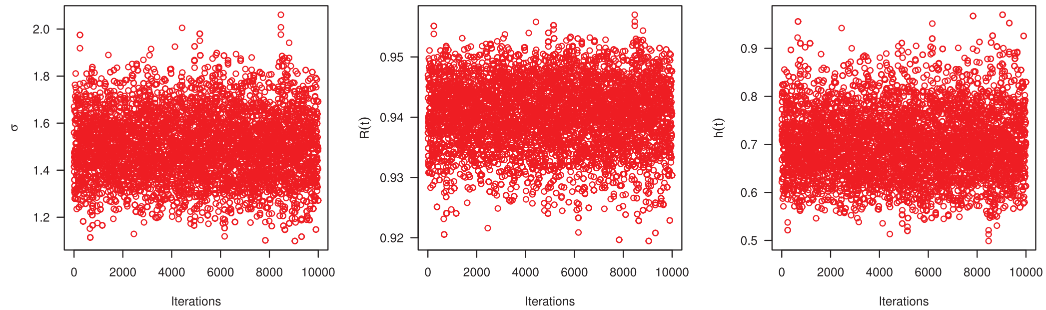

(d) Trace for Bayes-SF

Figure 5: The ACF and Trace diagrams of σ, $R(t)$, and $h(t)$ in Monte Carlo simulation

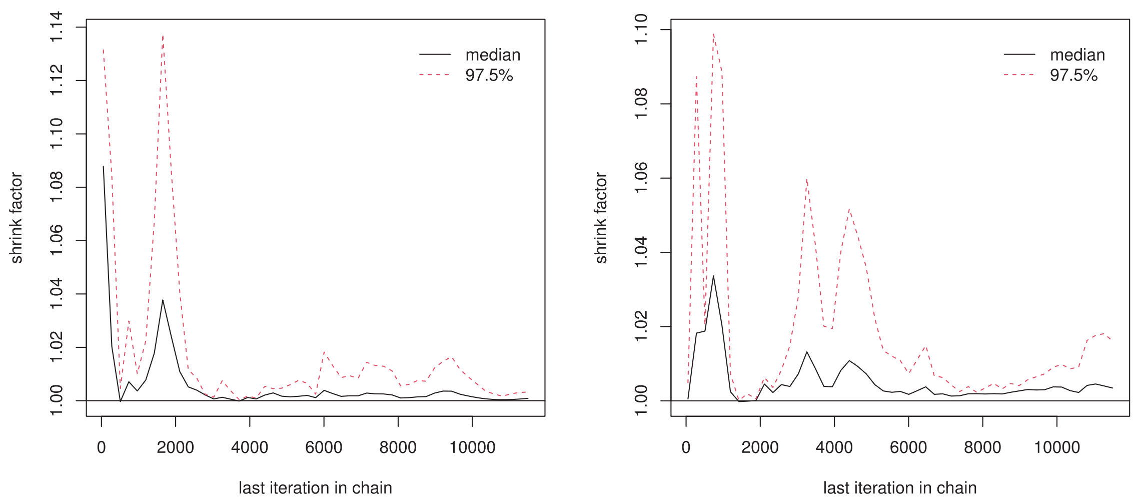

Figure 6: The BGR diagrams for two Bayes approaches in Monte Carlo simulation

Specifically, the average estimate (AE), root mean squared error (RMSE), mean relative absolute bias (MRAB), average confidence length (ACL), and coverage percentage (CP) of σ are given by

$$\mathrm{AE}(\ddot{\sigma}) = \frac{1}{1000}\sum_{i=1}^{1000} \ddot{\sigma}^{(i)},$$

$$\mathrm{RMSE}(\ddot{\sigma}) = \sqrt{\frac{1}{1000}\sum_{i=1}^{1000} \left(\ddot{\sigma}^{(i)} - \sigma\right)^2},$$

$$\mathrm{MRAB}(\ddot{\sigma}) = \frac{1}{1000}\sum_{i=1}^{1000} \sigma^{-1}\left|\ddot{\sigma}^{(i)} - \sigma\right|,$$

$$\mathrm{ACL}_{(1-\zeta)\%}(\sigma) = \frac{1}{1000}\sum_{i=1}^{1000} \left(\mathcal{U}_{\ddot{\sigma}^{(i)}} - \mathcal{L}_{\dot{\sigma}^{(i)}}\right),$$

and

$$\mathrm{CP}_{(1-\zeta)\%}(\sigma) = \frac{1}{1000}\sum_{i=1}^{1000} \boldsymbol{q}_{\left(\mathcal{L}_{\ddot{\sigma}^{(i)}};\mathcal{U}_{\check{\sigma}^{(i)}}\right)}(\sigma),$$

where $\ddot{\sigma}^{(i)}$ is the estimate of σ at ith sample, $\boldsymbol{q}(\cdot)$ is the indicator operator, $(\mathcal{L}(\cdot), \mathcal{U}(\cdot))$ refers to the (lower,upper) limits of $(1-\zeta)\%$ ACI (or HPD) interval of σ. Similarly, the AE, RMSE, MRAB, ACL, and CP values of $R(t)$ or $h(t)$ can be easily obtained.

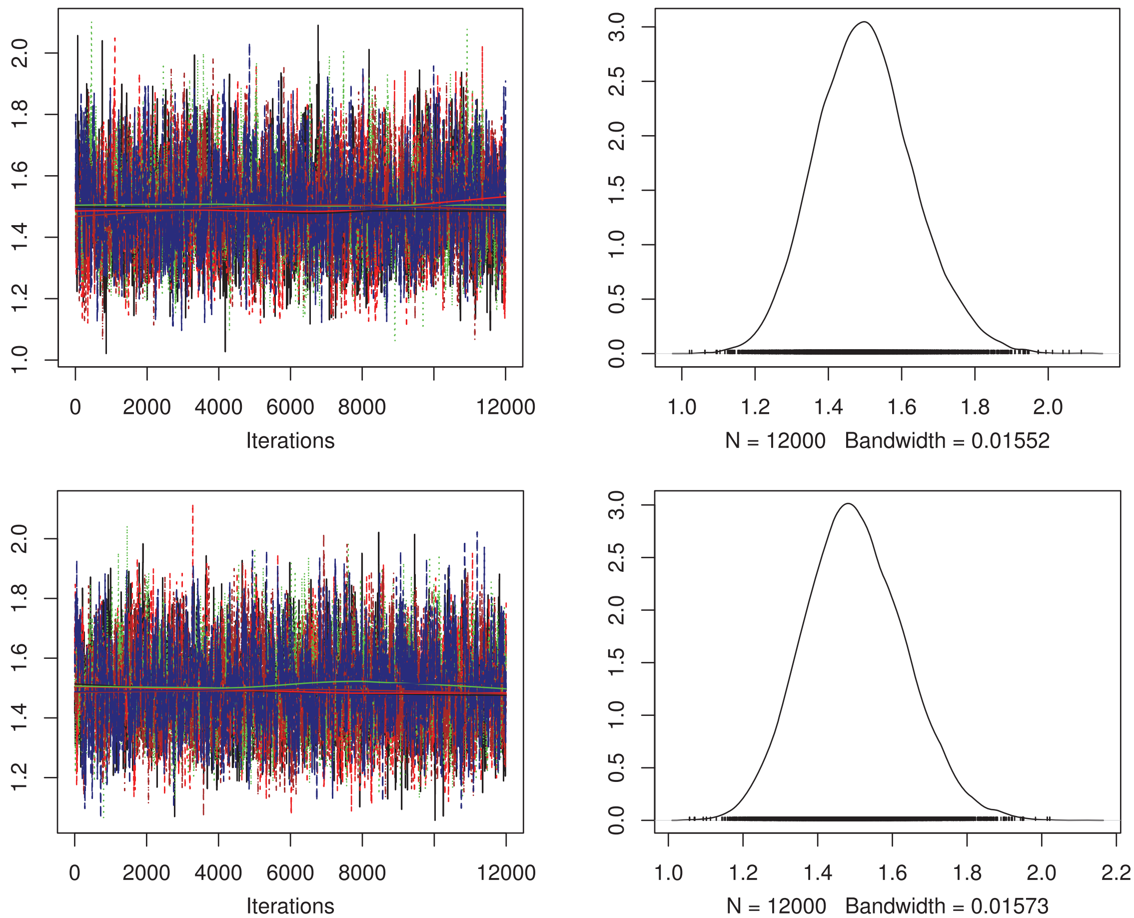

Figure 7: Trace and Density (along its Gaussian kernel) plots of σ from Bayes-LF (top) and Bayes-SF (bottom) approaches in Monte Carlo simulation

5.2 Simulation Outputs

From Tables 1–12, in terms of the lowest RMSE, MRAB, and ACL values, as well as the highest CP values, we will list different evaluations of how well the suggested approaches to estimating points and intervals perform on the unknown quantity subjects, such as:

- All the calculated estimates have shown good results of σ, $R(t)$, or $h(t)$ with respect all given accuracy criteria.
- As n increases, the estimated values of σ, $R(t)$, or $h(t)$ are highly good. We see the same behavior when $\sum_{i=1}^{m} R_i$ (or $n-m$) decreases.
- As T_i for $i = 1, 2$ grow, the simulated RMSE, MRAB, and ACL values narrowed down for all offered point (or interval) estimates of σ, $R(t)$, or $h(t)$ while their simulated CP values are increase.

- The Bayesian estimator generally outperforms the MLE in small sample sizes, showing lower bias, reduced RMSE, and coverage probabilities closer to the nominal level. This improved performance stems from the Bayesian method's ability to incorporate prior information, providing more stable estimates in finite samples.
- As σ increases, it is noted that
  - The RMSE, MRAB, and ACL values of σ increase except their CP values decrease.
  - The RMSE, MRAB, and ACL values of $R(t)$ or $h(t)$ decrease except their CP values increase.
- Comparing the proposed PT2C patterns 1, 2, and 3, all estimates of σ, $R(t)$, or $h(t)$ behave better based on Scheme-3 than others.
- Comparing the proposed estimation methodologies of σ, $R(t)$, and $h(t)$, it is observed that
  - Estimates of σ developed by maximum likelihood and Bayes-LF approaches are more accurate, significant, and better than those developed by others.
  - Estimates of $R(t)$ or $h(t)$ developed by the product of spacing and Bayes-SF approaches are more accurate, significant, and better than those developed by others.
- We recommend that, to obtain reliable findings for any parameter of life, the practitioner conducting the study extend the test for as long as feasible if and only if the study cost is sufficient.
- In short, if one aims to use data from Type-II improved adaptive progressive censored strategy, we suggest utilizing the Bayes approach using likelihood-based to estimate the model parameter and the Bayes approach using spacing-based to estimate the reliability indices of the unit-half-normal model.

Table 1: The Av.Es (1^{st} Col.), RMSEs (2^{nd} Col.), and MRABs (3^{rd} Col.) of σ when $\sigma = 1.5$

(T_1, T_2)	n[FP%]	Scheme	MLE			MPSE			Bayes-LF			Bayes-SF		
(0.2, 0.3)	50[50%]	1	1.7340	0.6182	0.3392	1.7821	0.6226	0.3441	1.4873	0.2185	0.1187	1.5398	0.2273	0.1192
		2	1.6850	0.5910	0.2609	1.7290	0.6124	0.2995	1.5030	0.2172	0.1162	1.5512	0.2263	0.1184
		3	1.6776	0.5734	0.2436	1.7225	0.5883	0.2467	1.5050	0.2146	0.1146	1.5520	0.2252	0.1179
	50[80%]	1	1.6477	0.5261	0.2372	1.6842	0.5370	0.2387	1.4875	0.2145	0.1134	1.5308	0.2221	0.1179
		2	1.6239	0.5217	0.2251	1.6566	0.5358	0.2274	1.4756	0.2134	0.1125	1.5158	0.2169	0.1141
		3	1.6381	0.5166	0.2110	1.6727	0.5341	0.2192	1.4584	0.2101	0.1117	1.4979	0.2125	0.1121
	80[50%]	1	1.6129	0.5158	0.2083	1.6451	0.5291	0.2147	1.4677	0.2098	0.1111	1.5055	0.2109	0.1119
		2	1.6344	0.4538	0.2073	1.6616	0.4621	0.2085	1.4652	0.2093	0.1108	1.5057	0.2090	0.1112
		3	1.6208	0.4132	0.1920	1.6484	0.4202	0.1932	1.4551	0.2068	0.1095	1.4970	0.2071	0.1107
	80[80%]	1	1.5948	0.3788	0.1768	1.6171	0.3880	0.1784	1.4888	0.2049	0.1089	1.5406	0.2070	0.1091
		2	1.5762	0.3749	0.1674	1.5962	0.3845	0.1687	1.4288	0.2038	0.1060	1.4722	0.2057	0.1086
		3	1.5839	0.3740	0.1593	1.6049	0.3809	0.1618	1.4662	0.1993	0.1050	1.5150	0.2029	0.1085
(0.4, 0.6)	50[50%]	1	1.1913	0.5183	0.2396	1.2669	0.5518	0.3374	1.4568	0.1701	0.0920	1.5316	0.1952	0.1076
		2	1.7321	0.4950	0.2312	1.7840	0.5157	0.2652	1.5074	0.1545	0.0826	1.5573	0.1791	0.0972
		3	1.6299	0.4506	0.2034	1.7035	0.4749	0.2179	1.5201	0.1341	0.0713	1.5897	0.1591	0.0865
	50[80%]	1	1.5591	0.3878	0.1981	1.5933	0.3984	0.2092	1.5106	0.1309	0.0707	1.5495	0.1533	0.0815
		2	1.7630	0.3418	0.1939	1.7963	0.3496	0.2042	1.6169	0.1301	0.0695	1.6484	0.1476	0.0778
		3	1.6094	0.3215	0.1763	1.6454	0.3380	0.1868	1.5427	0.1285	0.0682	1.5808	0.1469	0.0765
	80[50%]	1	1.5581	0.2879	0.1433	1.5924	0.3126	0.1646	1.5336	0.1278	0.0680	1.5696	0.1445	0.0762
		2	1.6219	0.2395	0.1187	1.6546	0.2389	0.1221	1.4889	0.1270	0.0673	1.5266	0.1354	0.0714
		3	1.6544	0.1911	0.0919	1.7050	0.2176	0.0986	1.5951	0.1239	0.0657	1.6308	0.1297	0.0679

(Continued)

Table 1 (continued)

(T_1, T_2)	n[FP%]	Scheme	MLE			MPSE			Bayes-LF			Bayes-SF		
	80[80%]	1	1.5328	0.1788	0.0856	1.5542	0.1892	0.0910	1.4473	0.1232	0.0646	1.4915	0.1278	0.0676
		2	1.7612	0.1465	0.0729	1.7821	0.1632	0.0751	1.5758	0.1177	0.0619	1.6141	0.1171	0.0635
		3	1.5827	0.1292	0.0648	1.6053	0.1352	0.0671	1.5132	0.1046	0.0552	1.5484	0.1144	0.0605

Table 2: The Av.Es (1st Col.), RMSEs (2nd Col.), and MRABs (3rd Col.) of σ when $\sigma = 2.5$

(T_1, T_2)	n[FP%]	Scheme	MLE			MPSE			Bayes-LF			Bayes-SF		
(0.3, 0.4)	50[50%]	1	2.7859	1.2496	0.3074	2.8646	1.2614	0.3119	2.4720	0.2436	0.0788	2.5597	0.2583	0.0814
		2	2.7943	1.2008	0.2841	2.8650	1.2123	0.2857	2.5164	0.2405	0.0775	2.6028	0.2563	0.0798
		3	2.7906	1.1429	0.2614	2.8627	1.1734	0.2685	2.5164	0.2383	0.0771	2.6028	0.2455	0.0781
	50[80%]	1	2.7814	0.9588	0.2485	2.8191	0.9681	0.2502	2.4660	0.2369	0.0764	2.5370	0.2415	0.0758
		2	2.7254	0.9396	0.2427	2.7798	0.9649	0.2444	2.4415	0.2363	0.0752	2.5107	0.2375	0.0756
		3	2.7625	0.9377	0.2298	2.7985	0.9631	0.2332	2.4665	0.2352	0.0745	2.5356	0.2358	0.0748
	80[50%]	1	2.6904	0.9071	0.2284	2.7440	0.9255	0.2330	2.4320	0.2342	0.0744	2.5040	0.2353	0.0746
		2	2.7033	0.8143	0.2221	2.7468	0.8299	0.2240	2.4745	0.2318	0.0742	2.5381	0.2336	0.0743
		3	2.6911	0.7410	0.2038	2.7351	0.7545	0.2057	2.4745	0.2302	0.0738	2.5381	0.2343	0.0742
	80[80%]	1	2.6830	0.6743	0.1877	2.7209	0.6988	0.1889	2.4573	0.2285	0.0733	2.5300	0.2332	0.0735
		2	2.6309	0.6684	0.1820	2.6643	0.6835	0.1833	2.3978	0.2275	0.0729	2.4677	0.2322	0.0731
		3	2.6541	0.6567	0.1771	2.6897	0.6776	0.1786	2.4746	0.2248	0.0720	2.5438	0.2275	0.0726
(0.5, 0.7)	50[50%]	1	2.6387	0.9791	0.3177	2.7284	1.0245	0.3030	2.4974	0.2419	0.0778	2.5869	0.2450	0.0801
		2	3.0514	0.8786	0.2915	3.1352	0.8390	0.2808	2.5008	0.2348	0.0754	2.5855	0.2389	0.0786
		3	2.1630	0.7972	0.2837	2.2930	0.8187	0.2512	2.4165	0.2317	0.0720	2.5452	0.2349	0.0779
	50[80%]	1	2.6026	0.7746	0.2115	2.6583	0.7200	0.2290	2.5400	0.2271	0.0702	2.6040	0.2325	0.0780
		2	2.9634	0.5649	0.2009	3.0179	0.6086	0.2137	2.6915	0.2203	0.0699	2.7548	0.2307	0.0760
		3	2.6790	0.5132	0.1885	2.7371	0.5427	0.2009	2.5657	0.2182	0.0690	2.6322	0.2272	0.0759
	80[50%]	1	2.6012	0.4174	0.1137	2.6569	0.4519	0.1228	2.5255	0.2158	0.0688	2.5917	0.2249	0.0756
		2	2.8638	0.3248	0.0953	2.9160	0.3409	0.1096	2.5493	0.2154	0.0680	2.6072	0.2235	0.0752
		3	2.0284	0.3141	0.0905	2.1270	0.3350	0.1023	2.2259	0.2144	0.0677	2.3090	0.2212	0.0741
	80[80%]	1	2.5638	0.3062	0.0882	2.5987	0.3335	0.0952	2.4173	0.2092	0.0661	2.4824	0.2130	0.0676
		2	2.9515	0.2379	0.0704	2.9858	0.2480	0.0843	2.6019	0.1896	0.0600	2.6604	0.2040	0.0650
		3	2.6287	0.2264	0.0664	2.6650	0.2473	0.0723	2.4984	0.1775	0.0568	2.5590	0.1873	0.0594

Table 3: The Av.Es (1st Col.), RMSEs (2nd Col.), and MRABs (3rd Col.) of $R(t)$ when $\sigma = 1.5$

(T_1, T_2)	n[FP%]	Scheme	MLE			MPSE			Bayes-LF			Bayes-SF		
(0.2, 0.3)	50[50%]	1	0.9419	0.0193	0.0169	0.9437	0.0184	0.0162	0.9399	0.0065	0.0055	0.9420	0.0058	0.0051
		2	0.9443	0.0179	0.0142	0.9458	0.0153	0.0133	0.9406	0.0062	0.0051	0.9424	0.0056	0.0048
		3	0.9440	0.0151	0.0129	0.9457	0.0146	0.0125	0.9406	0.0061	0.0050	0.9425	0.0055	0.0047
	50[80%]	1	0.9413	0.0148	0.0126	0.9427	0.0144	0.0123	0.9399	0.0060	0.0049	0.9416	0.0056	0.0047
		2	0.9416	0.0144	0.0119	0.9428	0.0135	0.0115	0.9394	0.0059	0.0049	0.9411	0.0055	0.0047
		3	0.9414	0.0135	0.0115	0.9427	0.0132	0.0112	0.9387	0.0059	0.0049	0.9404	0.0054	0.0047
	80[50%]	1	0.9407	0.0126	0.0107	0.9420	0.0124	0.0098	0.9391	0.0058	0.0048	0.9407	0.0055	0.0046
		2	0.9439	0.0125	0.0105	0.9449	0.0123	0.0105	0.9391	0.0058	0.0048	0.9407	0.0054	0.0046
		3	0.9433	0.0122	0.0102	0.9443	0.0121	0.0098	0.9386	0.0057	0.0048	0.9404	0.0055	0.0046
	80[80%]	1	0.9410	0.0118	0.0100	0.9418	0.0116	0.0098	0.9400	0.0057	0.0048	0.9420	0.0053	0.0045

(Continued)

Table 3 (continued)

(T_1, T_2)	n[FP%]	Scheme	MLE			MPSE			Bayes-LF			Bayes-SF		
		2	0.9412	0.0103	0.0087	0.9420	0.0102	0.0085	0.9375	0.0056	0.0047	0.9393	0.0053	0.0045
		3	0.9411	0.0100	0.0081	0.9419	0.0099	0.0080	0.9391	0.0055	0.0046	0.9411	0.0053	0.0044
(0.4, 0.6)	50[50%]	1	0.9181	0.0131	0.0142	0.9235	0.0163	0.0138	0.9388	0.0065	0.0053	0.9418	0.0058	0.0049
		2	0.9460	0.0129	0.0121	0.9477	0.0123	0.0113	0.9408	0.0060	0.0050	0.9427	0.0057	0.0047
		3	0.9435	0.0124	0.0115	0.9462	0.0120	0.0108	0.9413	0.0054	0.0048	0.9439	0.0053	0.0047
	50[80%]	1	0.9426	0.0117	0.0103	0.9439	0.0112	0.0108	0.9410	0.0053	0.0046	0.9425	0.0052	0.0045
		2	0.9488	0.0108	0.0100	0.9498	0.0105	0.0104	0.9449	0.0052	0.0045	0.9459	0.0051	0.0043
		3	0.9446	0.0105	0.0099	0.9458	0.0103	0.0100	0.9422	0.0051	0.0045	0.9436	0.0050	0.0042
	80[50%]	1	0.9425	0.0098	0.0073	0.9438	0.0093	0.0071	0.9419	0.0051	0.0043	0.9432	0.0049	0.0041
		2	0.9437	0.0066	0.0060	0.9449	0.0064	0.0055	0.9401	0.0049	0.0042	0.9416	0.0048	0.0041
		3	0.9451	0.0063	0.0053	0.9469	0.0059	0.0049	0.9441	0.0048	0.0041	0.9454	0.0047	0.0041
	80[80%]	1	0.9418	0.0061	0.0050	0.9427	0.0057	0.0047	0.9385	0.0047	0.0041	0.9403	0.0047	0.0041
		2	0.9491	0.0050	0.0042	0.9497	0.0047	0.0039	0.9435	0.0046	0.0038	0.9449	0.0045	0.0040
		3	0.9438	0.0047	0.0039	0.9446	0.0045	0.0037	0.9412	0.0042	0.0037	0.9425	0.0040	0.0034

Table 4: The Av.Es (1^{st} Col.), RMSEs (2^{nd} Col.), and MRABs (3^{rd} Col.) of $R(t)$ when $\sigma = 2.5$

(T_1, T_2)	n[FP%]	Scheme	MLE			MPSE			Bayes-LF			Bayes-SF		
(0.3, 0.4)	50[50%]	1	0.9641	0.0117	0.0096	0.9653	0.0110	0.0092	0.9638	0.0039	0.0032	0.9651	0.0037	0.0028
		2	0.9659	0.0101	0.0090	0.9669	0.0098	0.0083	0.9645	0.0038	0.0031	0.9657	0.0036	0.0028
		3	0.9659	0.0096	0.0082	0.9669	0.0093	0.0079	0.9645	0.0037	0.0030	0.9657	0.0034	0.0028
	50[80%]	1	0.9647	0.0095	0.0080	0.9652	0.0092	0.0077	0.9637	0.0036	0.0029	0.9648	0.0033	0.0028
		2	0.9648	0.0089	0.0074	0.9655	0.0087	0.0072	0.9634	0.0036	0.0029	0.9644	0.0033	0.0028
		3	0.9648	0.0086	0.0072	0.9653	0.0084	0.0070	0.9638	0.0035	0.0028	0.9647	0.0033	0.0027
	80[50%]	1	0.9642	0.0083	0.0067	0.9650	0.0081	0.0065	0.9632	0.0035	0.0028	0.9643	0.0032	0.0027
		2	0.9658	0.0082	0.0065	0.9664	0.0079	0.0064	0.9639	0.0034	0.0028	0.9648	0.0032	0.0027
		3	0.9656	0.0080	0.0064	0.9662	0.0078	0.0063	0.9639	0.0034	0.0028	0.9648	0.0032	0.0027
	80[80%]	1	0.9646	0.0075	0.0063	0.9652	0.0074	0.0061	0.9636	0.0033	0.0027	0.9647	0.0031	0.0026
		2	0.9646	0.0067	0.0057	0.9650	0.0066	0.0055	0.9627	0.0033	0.0027	0.9638	0.0031	0.0026
		3	0.9646	0.0066	0.0054	0.9651	0.0065	0.0053	0.9639	0.0033	0.0027	0.9649	0.0030	0.0026
(0.5, 0.7)	50[50%]	1	0.9658	0.0114	0.0091	0.9669	0.0108	0.0089	0.9642	0.0037	0.0030	0.9655	0.0035	0.0029
		2	0.9690	0.0095	0.0088	0.9699	0.0091	0.0084	0.9643	0.0036	0.0028	0.9655	0.0034	0.0028
		3	0.9545	0.0089	0.0077	0.9574	0.0085	0.0073	0.9631	0.0035	0.0027	0.9649	0.0033	0.0027
	50[80%]	1	0.9655	0.0072	0.0064	0.9663	0.0069	0.0060	0.9649	0.0034	0.0026	0.9657	0.0032	0.0026
		2	0.9697	0.0070	0.0060	0.9703	0.0067	0.0057	0.9669	0.0033	0.0026	0.9676	0.0031	0.0026
		3	0.9667	0.0061	0.0056	0.9674	0.0059	0.0047	0.9652	0.0032	0.0026	0.9661	0.0030	0.0026
	80[50%]	1	0.9655	0.0047	0.0037	0.9663	0.0045	0.0035	0.9647	0.0031	0.0026	0.9656	0.0030	0.0025
		2	0.9675	0.0044	0.0033	0.9681	0.0042	0.0032	0.9650	0.0030	0.0026	0.9658	0.0029	0.0025
		3	0.9534	0.0038	0.0032	0.9558	0.0037	0.0031	0.9599	0.0029	0.0026	0.9614	0.0028	0.0024
	80[80%]	1	0.9652	0.0036	0.0031	0.9657	0.0035	0.0028	0.9631	0.0028	0.0024	0.9641	0.0028	0.0024
		2	0.9697	0.0033	0.0026	0.9701	0.0031	0.0024	0.9658	0.0027	0.0023	0.9665	0.0027	0.0022
		3	0.9661	0.0030	0.0024	0.9666	0.0028	0.0022	0.9643	0.0026	0.0021	0.9652	0.0025	0.0021

Table 5: The Av.Es (1^{st} Col.), RMSEs (2^{nd} Col.), and MRABs (3^{rd} Col.) of $h(t)$ when $\sigma = 1.5$

(T_1, T_2)	n[FP%]	Scheme	MLE			MPSE			Bayes-LF			Bayes-SF		
(0.2, 0.3)	50[50%]	1	0.6892	0.2167	0.2574	0.6653	0.2092	0.2422	0.7095	0.0824	0.0927	0.6838	0.0727	0.0820

(Continued)

Table 5 (continued)

(T_1, T_2)	n[FP%]	Scheme	MLE			MPSE			Bayes-LF			Bayes-SF		
		2	0.6565	0.1971	0.2302	0.6369	0.1904	0.2230	0.7071	0.0784	0.0872	0.6830	0.0722	0.0806
		3	0.6593	0.1890	0.2182	0.6390	0.1818	0.2101	0.7006	0.0761	0.0848	0.6776	0.0711	0.0798
	50[80%]	1	0.6950	0.1845	0.2132	0.6776	0.1787	0.2062	0.7092	0.0751	0.0838	0.6877	0.0703	0.0802
		2	0.6906	0.1727	0.2008	0.6750	0.1676	0.1941	0.7152	0.0742	0.0832	0.6949	0.0689	0.0787
		3	0.6929	0.1686	0.1934	0.6765	0.1646	0.1885	0.7242	0.0735	0.0832	0.7037	0.0684	0.0786
	80[50%]	1	0.7021	0.1590	0.1814	0.6859	0.1535	0.1771	0.7191	0.0728	0.0816	0.7000	0.0680	0.0783
		2	0.6602	0.1544	0.1769	0.6480	0.1526	0.1653	0.7199	0.0727	0.0811	0.6993	0.0678	0.0779
		3	0.6685	0.1500	0.1684	0.6556	0.1481	0.1643	0.7254	0.0722	0.0810	0.7036	0.0678	0.0778
	80[80%]	1	0.6979	0.1469	0.1672	0.6871	0.1437	0.1614	0.7081	0.0717	0.0807	0.6831	0.0668	0.0761
		2	0.6946	0.1370	0.1464	0.6848	0.1257	0.1424	0.7393	0.0698	0.0789	0.7166	0.0666	0.0757
		3	0.6964	0.1219	0.1356	0.6861	0.1221	0.1335	0.7194	0.0685	0.0777	0.6950	0.0657	0.0742
(0.4, 0.6)	50[50%]	1	0.9930	0.1788	0.2187	0.9226	0.1692	0.2142	0.7237	0.0805	0.0986	0.6858	0.0716	0.0862
		2	0.6355	0.1689	0.1928	0.6134	0.1601	0.1895	0.6985	0.0745	0.0900	0.6744	0.0711	0.0814
		3	0.6664	0.1553	0.1829	0.6326	0.1495	0.1805	0.6915	0.0688	0.0792	0.6591	0.0674	0.0787
	50[80%]	1	0.6760	0.1385	0.1804	0.6602	0.1321	0.1724	0.6959	0.0660	0.0768	0.6775	0.0655	0.0762
		2	0.5993	0.1296	0.1735	0.5870	0.1260	0.1671	0.6472	0.0654	0.0755	0.6342	0.0647	0.0749
		3	0.6510	0.1272	0.1674	0.6357	0.1248	0.1471	0.6803	0.0644	0.0735	0.6630	0.0637	0.0724
	80[50%]	1	0.6767	0.1188	0.1217	0.6609	0.1145	0.1193	0.6849	0.0637	0.0727	0.6683	0.0625	0.0717
		2	0.6626	0.0944	0.1084	0.6476	0.0794	0.0924	0.7069	0.0613	0.0712	0.6883	0.0611	0.0696
		3	0.6453	0.0833	0.0882	0.6230	0.0764	0.0852	0.6565	0.0609	0.0707	0.6412	0.0601	0.0690
	80[80%]	1	0.6850	0.0786	0.0794	0.6749	0.0716	0.0843	0.7271	0.0597	0.0693	0.7048	0.0586	0.0685
		2	0.5960	0.0657	0.0691	0.5883	0.0614	0.0705	0.6641	0.0578	0.0674	0.6476	0.0564	0.0650
		3	0.6606	0.0580	0.0655	0.6507	0.0558	0.0620	0.6932	0.0528	0.0617	0.6766	0.0515	0.0577

Table 6: The Av.Es (1^{st} Col.), RMSEs (2^{nd} Col.), and MRABs (3^{rd} Col.) of $h(t)$ when $\sigma = 2.5$

(T_1, T_2)	n[FP%]	Scheme	MLE			MPSE			Bayes-LF			Bayes-SF		
(0.3, 0.4)	50[50%]	1	0.4149	0.1398	0.2723	0.4009	0.1318	0.2595	0.4170	0.0469	0.0894	0.4020	0.0440	0.0832
		2	0.3924	0.1200	0.2402	0.3812	0.1171	0.2344	0.4091	0.0449	0.0857	0.3949	0.0424	0.0818
		3	0.3922	0.1142	0.2258	0.3807	0.1104	0.2197	0.4091	0.0438	0.0838	0.3949	0.0414	0.0798
	50[80%]	1	0.4077	0.1110	0.2213	0.4013	0.1087	0.2177	0.4180	0.0427	0.0832	0.4057	0.0395	0.0795
		2	0.4060	0.1059	0.2096	0.3971	0.1027	0.2020	0.4222	0.0426	0.0818	0.4101	0.0394	0.0780
		3	0.4067	0.1026	0.2014	0.4006	0.1004	0.1971	0.4177	0.0418	0.0813	0.4059	0.0384	0.0773
	80[50%]	1	0.4135	0.0983	0.1871	0.4042	0.0959	0.1835	0.4240	0.0417	0.0800	0.4113	0.0374	0.0768
		2	0.3938	0.0955	0.1859	0.3868	0.0935	0.1781	0.4162	0.0406	0.0792	0.4052	0.0363	0.0765
		3	0.3965	0.0946	0.1829	0.3893	0.0922	0.1762	0.4162	0.0406	0.0779	0.4052	0.0353	0.0762
	80[80%]	1	0.4079	0.0896	0.1754	0.4016	0.0877	0.1717	0.4192	0.0400	0.0769	0.4068	0.0347	0.0750
		2	0.4087	0.0798	0.1589	0.4030	0.0783	0.1548	0.4300	0.0392	0.0763	0.4174	0.0338	0.0741
		3	0.4085	0.0779	0.1523	0.4026	0.0769	0.1487	0.4161	0.0383	0.0753	0.4044	0.0332	0.0731
(0.5,0.7)	50[50%]	1	0.3940	0.1291	0.2353	0.3799	0.1239	0.2148	0.4119	0.0443	0.0864	0.3970	0.0414	0.0806
		2	0.3561	0.1137	0.2240	0.3447	0.1077	0.2092	0.4114	0.0418	0.0837	0.3973	0.0404	0.0798
		3	0.5313	0.1048	0.2150	0.4956	0.1011	0.1943	0.4260	0.0412	0.0823	0.4035	0.0392	0.0769
	50[80%]	1	0.3965	0.0950	0.1798	0.3876	0.0855	0.1680	0.4044	0.0398	0.0807	0.3941	0.0388	0.0758
		2	0.3471	0.0887	0.1688	0.3404	0.0789	0.1561	0.3806	0.0394	0.0783	0.3716	0.0375	0.0748
		3	0.3832	0.0795	0.1372	0.3746	0.0728	0.1227	0.4001	0.0376	0.0752	0.3895	0.0370	0.0734
	80[50%]	1	0.3967	0.0735	0.1028	0.3878	0.0690	0.0952	0.4069	0.0365	0.0727	0.3961	0.0357	0.0711
		2	0.3739	0.0713	0.0957	0.3661	0.0644	0.0903	0.4029	0.0361	0.0716	0.3936	0.0344	0.0701
		3	0.5433	0.0655	0.0877	0.5150	0.0572	0.0816	0.4637	0.0349	0.0707	0.4462	0.0332	0.0690

(Continued)

Table 6 (continued)

(T_1, T_2)	n[FP%]	Scheme	MLE			MPSE			Bayes-LF			Bayes-SF		
	80[80%]	1	0.4008	0.0542	0.0793	0.3951	0.0457	0.0759	0.4252	0.0342	0.0687	0.4136	0.0316	0.0660
		2	0.3465	0.0455	0.0753	0.3423	0.0360	0.0625	0.3936	0.0321	0.0677	0.3847	0.0302	0.0632
		3	0.3894	0.0387	0.0720	0.3838	0.0354	0.0584	0.4106	0.0304	0.0659	0.4005	0.0288	0.0589

Table 7: The ACLs (1st Col.) and CPs (2nd Col.) of 95% ACI/HPD estimates of σ when $\sigma = 1.5$

(T_1, T_2)	n[FP%]	Scheme	ACI-LF		ACI-SF		HPD-LF		HPD-SF	
(0.2, 0.3)	50[50%]	1	2.2606	0.896	2.3716	0.887	0.5607	0.982	0.5697	0.979
		2	2.1053	0.902	2.2053	0.893	0.5516	0.984	0.5591	0.980
		3	1.9802	0.908	2.1320	0.899	0.5457	0.985	0.5572	0.981
	50[80%]	1	1.9243	0.913	2.0698	0.905	0.5341	0.987	0.5515	0.982
		2	1.8953	0.918	2.0034	0.910	0.5321	0.987	0.5424	0.982
		3	1.8693	0.925	1.9740	0.916	0.5313	0.988	0.5414	0.983
(0.4, 0.6)	80[50%]	1	1.7844	0.928	1.8924	0.919	0.5273	0.989	0.5384	0.984
		2	1.6704	0.932	1.7771	0.923	0.5227	0.990	0.5359	0.985
		3	1.5464	0.936	1.6526	0.928	0.5176	0.991	0.5350	0.986
	80[80%]	1	1.4339	0.940	1.5485	0.931	0.5106	0.992	0.5290	0.987
		2	1.4093	0.943	1.4609	0.934	0.5008	0.994	0.5114	0.990
		3	1.3738	0.945	1.4114	0.937	0.4953	0.995	0.5042	0.991
(0.2,0.3)	50[50%]	1	1.2522	0.918	1.3412	0.909	0.5193	0.985	0.5292	0.982
		2	1.1733	0.925	1.2722	0.915	0.4949	0.987	0.5125	0.983
		3	1.0203	0.931	1.1303	0.920	0.4904	0.988	0.4917	0.984
	50[80%]	1	1.0159	0.934	1.0666	0.926	0.4856	0.990	0.4890	0.986
		2	0.9312	0.938	0.9754	0.932	0.4819	0.990	0.4848	0.986
		3	0.9166	0.946	0.9654	0.937	0.4781	0.991	0.4811	0.987
(0.4,0.6)	80[50%]	1	0.9161	0.951	0.9648	0.942	0.4754	0.992	0.4802	0.987
		2	0.8879	0.955	0.9363	0.946	0.4715	0.993	0.4764	0.988
		3	0.8289	0.958	0.8700	0.950	0.4678	0.994	0.4735	0.989
	80[80%]	1	0.8029	0.962	0.8256	0.953	0.4172	0.995	0.4485	0.991
		2	0.7080	0.967	0.7319	0.957	0.4040	0.997	0.4338	0.993
		3	0.6864	0.969	0.7101	0.961	0.4020	0.998	0.4133	0.994

Table 8: The ACLs (1st Col.) and CPs (2nd Col.) of 95% ACI/HPD estimates of σ when $\sigma = 2.5$

(T_1, T_2)	n[FP%]	Scheme	ACI-LF		ACI-SF		HPD-LF		HPD-SF	
(0.3, 0.4)	50[50%]	1	4.1713	0.814	4.2419	0.810	0.9244	0.927	0.9309	0.922
		2	3.7824	0.835	3.8884	0.831	0.9208	0.928	0.9290	0.924
		3	3.5569	0.841	3.6531	0.836	0.9183	0.930	0.9259	0.925
	50[80%]	1	3.3504	0.842	3.5300	0.839	0.9164	0.932	0.9198	0.927
		2	3.3226	0.845	3.4504	0.841	0.9135	0.934	0.9170	0.929
		3	3.2791	0.848	3.4178	0.843	0.8995	0.937	0.9153	0.932
(0.5,0.7)	80[50%]	1	3.1257	0.850	3.2397	0.846	0.8932	0.940	0.9115	0.934
		2	2.7722	0.856	2.8562	0.852	0.8893	0.942	0.9109	0.937
		3	2.6572	0.858	2.7646	0.854	0.8867	0.943	0.9059	0.938
	80[80%]	1	2.4767	0.861	2.5621	0.857	0.8789	0.945	0.8969	0.940
		2	2.4535	0.863	2.5391	0.859	0.8699	0.946	0.8910	0.941
		3	2.3981	0.866	2.4636	0.862	0.8611	0.948	0.8810	0.943

(Continued)

Table 8 (continued)

(T_1, T_2)	n[FP%]	Scheme	ACI-LF		ACI-SF		HPD-LF		HPD-SF	
(0.3,0.4)	50[50%]	1	2.2554	0.847	2.4011	0.849	0.8693	0.929	0.8735	0.927
		2	2.0266	0.868	2.1929	0.857	0.8543	0.930	0.8663	0.928
		3	1.7608	0.875	1.8383	0.866	0.8247	0.932	0.8449	0.930
	50[80%]	1	1.6864	0.880	1.7582	0.870	0.8220	0.935	0.8445	0.931
		2	1.6187	0.883	1.7069	0.874	0.8136	0.937	0.8399	0.934
		3	1.5837	0.886	1.6652	0.877	0.8099	0.940	0.8378	0.937
(0.5,0.7)	80[50%]	1	1.5330	0.891	1.5613	0.882	0.8046	0.943	0.8188	0.940
		2	1.3815	0.899	1.5147	0.886	0.7990	0.945	0.8028	0.942
		3	1.2870	0.904	1.4197	0.892	0.7207	0.946	0.7330	0.944
	80[80%]	1	1.2297	0.913	1.3699	0.901	0.7187	0.948	0.7250	0.945
		2	1.1809	0.915	1.2204	0.906	0.7030	0.950	0.7180	0.947
		3	0.9150	0.918	1.1301	0.910	0.6888	0.952	0.7029	0.949

Table 9: The ACLs (1st Col.) and CPs (2nd Col.) of 95% ACI/HPD estimates of $R(t)$ when $\sigma = 1.5$

(T_1, T_2)	n[FP%]	Scheme	ACI-LF		ACI-SF		HPD-LF		HPD-SF	
(0.2,0.3)	50[50%]	1	0.0765	0.943	0.0760	0.944	0.0228	0.967	0.0216	0.969
		2	0.0675	0.948	0.0671	0.949	0.0226	0.968	0.0215	0.970
		3	0.0645	0.950	0.0642	0.951	0.0224	0.968	0.0214	0.970
	50[80%]	1	0.0640	0.951	0.0637	0.952	0.0222	0.970	0.0212	0.971
		2	0.0617	0.953	0.0605	0.954	0.0221	0.971	0.0210	0.973
		3	0.0591	0.955	0.0587	0.956	0.0220	0.971	0.0207	0.973
(0.4, 0.6)	80[50%]	1	0.0583	0.956	0.0579	0.957	0.0215	0.973	0.0205	0.974
		2	0.0540	0.958	0.0538	0.959	0.0214	0.973	0.0204	0.975
		3	0.0510	0.961	0.0509	0.962	0.0213	0.974	0.0203	0.976
	80[80%]	1	0.0484	0.964	0.0478	0.965	0.0212	0.975	0.0200	0.977
		2	0.0471	0.965	0.0469	0.966	0.0211	0.975	0.0195	0.978
		3	0.0468	0.967	0.0461	0.968	0.0207	0.976	0.0191	0.979
(0.2,0.3)	50[50%]	1	0.0421	0.953	0.0414	0.954	0.0213	0.971	0.0188	0.973
		2	0.0386	0.957	0.0381	0.958	0.0208	0.972	0.0182	0.974
		3	0.0350	0.960	0.0342	0.961	0.0194	0.973	0.0181	0.974
	50[80%]	1	0.0344	0.961	0.0339	0.962	0.0189	0.974	0.0180	0.976
		2	0.0335	0.963	0.0332	0.964	0.0188	0.975	0.0178	0.977
		3	0.0321	0.964	0.0318	0.966	0.0184	0.976	0.0173	0.978
(0.4, 0.6)	80[50%]	1	0.0305	0.966	0.0302	0.967	0.0177	0.977	0.0169	0.979
		2	0.0294	0.968	0.0292	0.969	0.0173	0.977	0.0168	0.979
		3	0.0273	0.970	0.0266	0.972	0.0168	0.978	0.0158	0.980
	80[80%]	1	0.0267	0.972	0.0263	0.973	0.0165	0.979	0.0156	0.980
		2	0.0248	0.973	0.0242	0.974	0.0156	0.980	0.0153	0.981
		3	0.0236	0.975	0.0230	0.976	0.0150	0.981	0.0148	0.982

Table 10: The ACLs (1st Col.) and CPs (2nd Col.) of 95% ACI/HPD estimates of $R(t)$ when $\sigma = 2.5$

(T_1, T_2)	n[FP%]	Scheme	ACI-LF		ACI-SF		HPD-LF		HPD-SF	
(0.3, 0.4)	50[50%]	1	0.0484	0.951	0.0480	0.953	0.0137	0.973	0.0131	0.974
		2	0.0432	0.955	0.0421	0.956	0.0136	0.973	0.0130	0.974

(Continued)

Table 10 (continued)

(T_1, T_2)	n[FP%]	Scheme	ACI-LF		ACI-SF		HPD-LF		HPD-SF	
		3	0.0411	0.958	0.0403	0.959	0.0135	0.974	0.0129	0.975
	50[80%]	1	0.0403	0.959	0.0399	0.960	0.0134	0.975	0.0128	0.976
		2	0.0381	0.961	0.0379	0.962	0.0133	0.976	0.0127	0.977
		3	0.0374	0.962	0.0372	0.963	0.0132	0.977	0.0126	0.978
(0.5,0.7)	80[50%]	1	0.0367	0.964	0.0361	0.965	0.0131	0.977	0.0125	0.978
		2	0.0336	0.966	0.0332	0.967	0.0130	0.978	0.0124	0.979
		3	0.0319	0.969	0.0310	0.969	0.0128	0.979	0.0123	0.980
	80[80%]	1	0.0309	0.971	0.0304	0.971	0.0127	0.980	0.0122	0.981
		2	0.0300	0.972	0.0297	0.973	0.0126	0.981	0.0121	0.981
		3	0.0298	0.974	0.0293	0.975	0.0125	0.981	0.0120	0.982
(0.3,0.4)	50[50%]	1	0.0273	0.959	0.0267	0.961	0.0129	0.970	0.0121	0.972
		2	0.0266	0.963	0.0252	0.965	0.0124	0.973	0.0118	0.974
		3	0.0242	0.966	0.0233	0.968	0.0123	0.975	0.0117	0.977
	50[80%]	1	0.0236	0.967	0.0211	0.969	0.0122	0.976	0.0115	0.978
		2	0.0226	0.969	0.0208	0.971	0.0116	0.978	0.0114	0.980
		3	0.0215	0.970	0.0202	0.972	0.0114	0.978	0.0113	0.979
(0.5,0.7)	80[50%]	1	0.0199	0.972	0.0190	0.974	0.0113	0.979	0.0111	0.981
		2	0.0189	0.974	0.0185	0.976	0.0110	0.980	0.0105	0.982
		3	0.0179	0.977	0.0172	0.979	0.0109	0.982	0.0103	0.983
	80[80%]	1	0.0165	0.979	0.0161	0.981	0.0100	0.984	0.0099	0.984
		2	0.0151	0.980	0.0145	0.982	0.0098	0.985	0.0096	0.986
		3	0.0142	0.982	0.0138	0.984	0.0094	0.986	0.0092	0.987

Table 11: The ACLs (1^{st} Col.) and CPs (2^{nd} Col.) of 95% ACI/HPD estimates of $h(t)$ when $\sigma = 1.5$

(T_1, T_2)	n[FP%]	Scheme	ACI-LF		ACI-SF		HPD-LF		HPD-SF	
(0.2,0.3)	50[50%]	1	0.9681	0.918	0.9537	0.920	0.2824	0.957	0.2707	0.959
		2	0.8425	0.926	0.8405	0.928	0.2793	0.959	0.2691	0.961
		3	0.8067	0.930	0.8052	0.932	0.2781	0.960	0.2667	0.962
	50[80%]	1	0.7984	0.931	0.7965	0.934	0.2779	0.960	0.2648	0.962
		2	0.7575	0.935	0.7558	0.937	0.2769	0.961	0.2627	0.963
		3	0.7325	0.938	0.7299	0.940	0.2751	0.962	0.2589	0.964
(0.4, 0.6)	80[50%]	1	0.7219	0.940	0.7191	0.942	0.2696	0.964	0.2584	0.965
		2	0.6743	0.944	0.6733	0.946	0.2683	0.965	0.2543	0.967
		3	0.6374	0.947	0.6316	0.949	0.2671	0.966	0.2511	0.970
	80[80%]	1	0.6083	0.950	0.6035	0.952	0.2653	0.969	0.2504	0.972
		2	0.5867	0.952	0.5826	0.954	0.2637	0.971	0.2487	0.973
		3	0.5816	0.953	0.5804	0.955	0.2600	0.973	0.2478	0.975
(0.2,0.3)	50[50%]	1	0.5215	0.937	0.5157	0.939	0.2587	0.964	0.2336	0.967
		2	0.4779	0.941	0.4735	0.942	0.2567	0.966	0.2297	0.969
		3	0.4339	0.945	0.4258	0.947	0.2431	0.967	0.2276	0.970
	50[80%]	1	0.4167	0.948	0.4138	0.950	0.2353	0.967	0.2253	0.970
		2	0.4163	0.949	0.4133	0.950	0.2345	0.968	0.2219	0.971
		3	0.3980	0.952	0.3958	0.952	0.2291	0.969	0.2182	0.972
(0.4, 0.6)	80[50%]	1	0.3773	0.955	0.3745	0.956	0.2201	0.971	0.2101	0.973
		2	0.3613	0.957	0.3592	0.958	0.2173	0.972	0.2059	0.974
		3	0.3326	0.960	0.3312	0.961	0.2080	0.973	0.2020	0.975
	80[80%]	1	0.3300	0.962	0.3260	0.964	0.2042	0.976	0.1955	0.978
		2	0.3050	0.965	0.3001	0.966	0.1953	0.978	0.1910	0.979

(Continued)

Table 11 (continued)

(T_1, T_2)	n[FP%]	Scheme	ACI-LF		ACI-SF		HPD-LF		HPD-SF	
		3	0.2873	0.969	0.2817	0.970	0.1866	0.980	0.1830	0.981

Table 12: The ACLs (1st Col.) and CPs (2nd Col.) of 95% ACI/HPD estimates of $h(t)$ when $\sigma = 2.5$

(T_1, T_2)	n[FP%]	Scheme	ACI-LF		ACI-SF		HPD-LF		HPD-SF	
(0.3, 0.4)	50[50%]	1	0.5314	0.937	0.5256	0.939	0.1683	0.961	0.1596	0.963
		2	0.5086	0.941	0.5018	0.942	0.1645	0.962	0.1574	0.964
		3	0.4873	0.944	0.4795	0.946	0.1619	0.964	0.1540	0.965
	50[80%]	1	0.4773	0.946	0.4676	0.948	0.1598	0.965	0.1528	0.967
		2	0.4580	0.948	0.4527	0.950	0.1583	0.966	0.1516	0.968
		3	0.4494	0.950	0.4426	0.952	0.1569	0.968	0.1507	0.970
(0.5,0.7)	80[50%]	1	0.4386	0.953	0.4260	0.955	0.1564	0.969	0.1501	0.970
		2	0.4080	0.956	0.3933	0.958	0.1542	0.971	0.1493	0.973
		3	0.3882	0.959	0.3805	0.961	0.1522	0.973	0.1456	0.974
	80[80%]	1	0.3762	0.961	0.3616	0.963	0.1505	0.975	0.1446	0.976
		2	0.3653	0.963	0.3526	0.965	0.1486	0.976	0.1434	0.978
		3	0.3522	0.965	0.3451	0.967	0.1453	0.978	0.1414	0.979
(0.3,0.4)	50[50%]	1	0.3245	0.946	0.3149	0.948	0.1554	0.967	0.1457	0.969
		2	0.3128	0.948	0.3049	0.950	0.1515	0.968	0.1396	0.970
		3	0.2760	0.952	0.2651	0.954	0.1471	0.970	0.1364	0.972
	50[80%]	1	0.2572	0.954	0.2513	0.956	0.1459	0.970	0.1353	0.972
		2	0.2475	0.956	0.2456	0.958	0.1383	0.971	0.1327	0.973
		3	0.2414	0.957	0.2346	0.959	0.1353	0.973	0.1319	0.974
(0.5,0.7)	80[50%]	1	0.2337	0.959	0.2236	0.961	0.1331	0.974	0.1318	0.974
		2	0.2270	0.962	0.2216	0.964	0.1311	0.975	0.1244	0.977
		3	0.2165	0.964	0.2098	0.967	0.1263	0.978	0.1205	0.980
	80[80%]	1	0.1995	0.967	0.1926	0.969	0.1218	0.980	0.1179	0.981
		2	0.1852	0.969	0.1794	0.972	0.1171	0.981	0.1143	0.982
		3	0.1766	0.972	0.1658	0.975	0.1120	0.982	0.1102	0.983

A heatmap is a tool that displays information in a visual manner. Fig. 8 demonstrates some estimation outcomes of σ (as an example). In each heatmap, the estimation methods are putted on the 'x-axis' line whereas the proposed censoring settings (denoted by $[T_1, T_2] - n[\mathrm{FP}\%] - \mathrm{PT2C}$) are putted on the 'y-axis' line. Fig. 8 supports the same numerical findings listed in Tables 1–12.

6 Shasta Reservoir Data Analysis

Shasta reservoir, with a gross pool storage capacity of 4,552,000 acre-feet, is California's biggest man-made lake. It provides a lake for long-term water storage, flood control, hydroelectricity, and saline water protection. This section presents various inferential analyses of information about how much water is in the Shasta reservoir in California each month in February between 1991 and 2010. Nadar et al. [29] transformed the actual water capacity data set into bounded data in the interval [0, 1]; see Table 13.

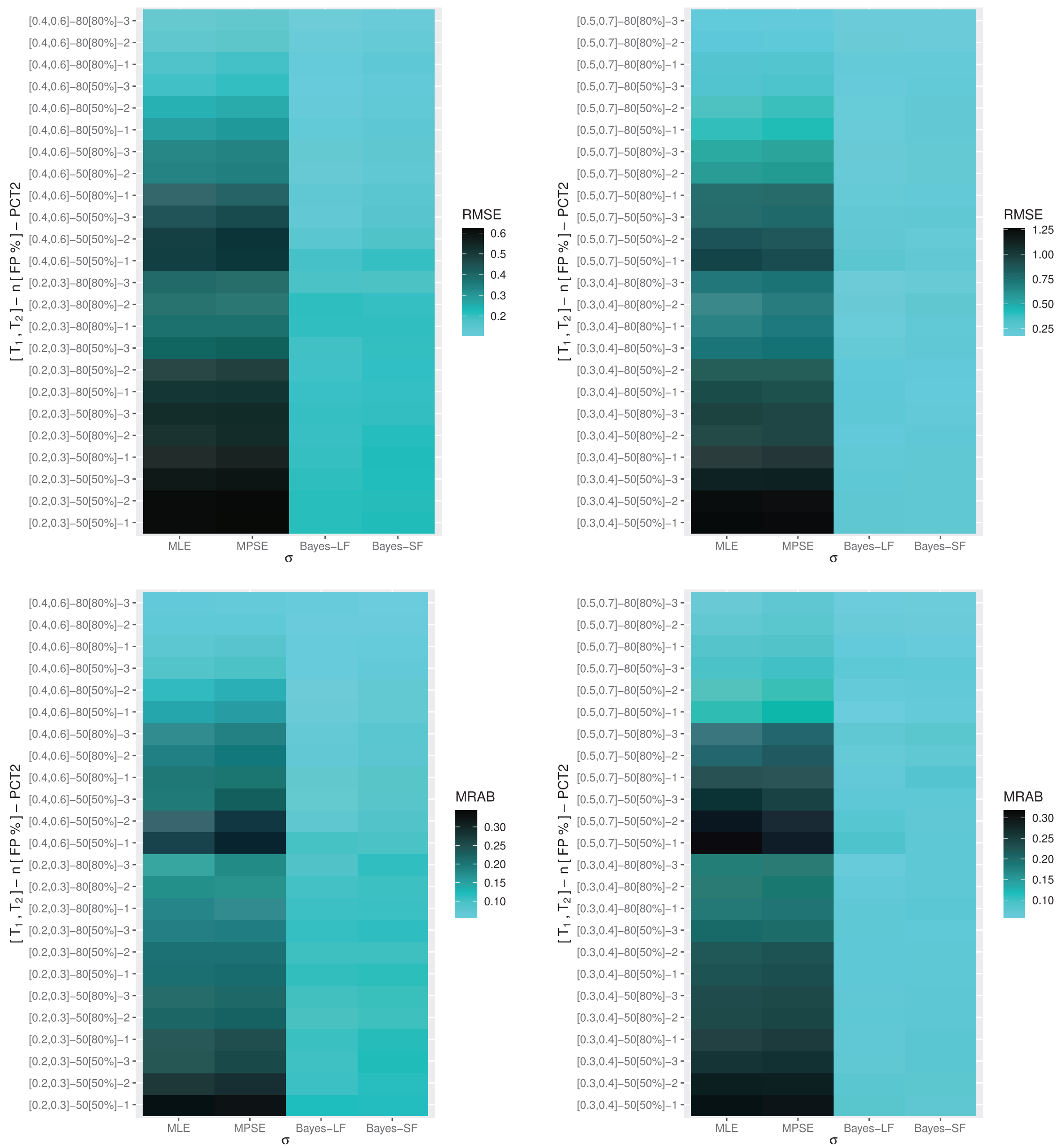

(a) $\sigma = 1\ 5$ (b) $\sigma = 2\ 5$

Figure 8: Heatmaps for the RMSE and MRAB results of σ

Table 13: Monthly water capacity data for Shasta reservoir

0.338936	0.430681	0.431915	0.580194	0.695970	0.724626	0.742563	0.757583	0.759932	0.768007
0.783660	0.785339	0.787408	0.811556	0.815627	0.828689	0.842316	0.843485	0.847413	0.849868

To highlight the importance of the UHN model, based on the Shasta reservoir data, we'll compare it with nine other models, including:

(1) Unit–log–log (ULL(σ)) by Korkmaz and Korkmaz [30];
(2) Unit–Birnbaum–Saunders (UBS(ρ,σ)) by Mazucheli et al. [31];
(3) Unit–Gompertz (UGom(ρ,σ)) by Mazucheli et al. [32];
(4) Unit–Weibull (UW(ρ,σ)) by Mazucheli et al. [33];
(5) Unit–gamma (UG(ρ,σ)) by Mazucheli et al. [34];
(6) Topp–Leone (TL(ρ)) by Topp and Leone [35];
(7) Unit–Lindley (UL(σ)) by Mazucheli et al. [36];
(8) Kumaraswamy (Kum(ρ,σ)) by Mitnik and Baek [37];
(9) Beta (Beta(ρ,σ)) by Gupta and Nadarajah [38].

To specific the best model, we consider the different criteria namely: (i) log-likelihood value (say, $\mathcal{L}^\bullet$); (ii) Akaike (say, $\mathcal{A}$); (iii) Consistent Akaike (say, $\mathcal{CA}$); (iv) Bayesian (say, $\mathcal{B}$); (v) Hannan-Quinn (say, $\mathcal{HQ}$); (vi) Anderson-Darling (say, $\mathcal{AD}$); (vii) Cramér-von Mises (say, $\mathcal{CM}$); and (viii) Kolmogorov–Smirnov (say, $\mathcal{KS}$) along its $\wp$-Value. The optimum model is distinguished by having the lowest values for all goodness of fit measures, except the highest $\wp$-Value. From Table 13, Table 14 displays the MLEs (with their standard errors (SErrs)) of ρ and σ as well as the fitted values of the UHN and its competitors. Outcomes in Table 14 showed that the suggested UHN model is the best choice among others based on the criteria (i)–(vii), while the UBS model (by Mazucheli et al. [31]) produces the lowest $\mathcal{KS}$ distance with the largest $\wp$-Value.

Table 14: Outcomes for fitting of the UHN and its competitive models from Shasta reservoir data

Model	MLE(SErr)		$\mathcal{L}^\bullet$	$\mathcal{A}$	$\mathcal{CA}$	$\mathcal{B}$	$\mathcal{HQ}$	$\mathcal{AD}$	$\mathcal{CM}$	$\mathcal{KS}$($\wp$-Value)
	ρ	σ								
UHN	–	3.7200(0.5882)	−14.756	−27.512	−27.289	−26.516	−27.317	0.666	0.097	0.271(0.087)
ULL	5.0253(1.1192)	1.0375(0.1846)	−8.6847	−13.369	−12.664	−11.378	−12.981	2.220	0.405	0.274(0.081)
UBS	0.3052(0.0378)	0.5782(0.0914)	−14.712	−25.624	−24.918	−23.633	−25.235	1.217	0.201	0.217(0.262)
UGom	1.1604(0.7682)	1.6931(1.6275)	−8.8489	−13.698	−12.992	−11.706	−13.309	2.044	0.368	0.297(0.047)
UW	1.5704(0.2483)	4.2071(1.1202)	−10.957	−17.914	−17.208	−15.922	−17.525	1.874	0.332	0.242(0.164)
UG	8.1071(2.6544)	2.8787(0.8628)	−12.528	−21.056	−20.350	−19.065	−20.667	2.043	0.366	0.393(0.003)
TL	–	8.6668(1.9379)	−11.588	−21.175	−20.953	−20.180	−20.981	1.786	0.313	0.255(0.124)
UL	–	0.4957(0.0806)	−13.827	−25.654	−25.432	−24.659	−25.460	0.835	0.127	0.242(0.162)
Kum	4.4899(2.0414)	6.3480(1.5576)	−13.475	−22.949	−22.244	−20.958	−22.561	1.424	0.241	0.221(0.245)
Beta	2.9098(0.8754)	7.3155(2.3181)	−12.562	−21.124	−20.418	−19.132	−20.735	1.619	0.280	0.236(0.183)

We also represented different graphics; they displayed how well the fittings turned out, namely probability-probability (PP), which represents the relationship between observed cumulative probabilities (OCPs) and empirical cumulative probabilities (ECPs); see Fig. 9a; quantile-quantile (QQ); see Fig. 9b; data histograms with fitted density lines; see Fig. 9c; Fitted reliability lines; see Fig. 9d; Scaled–TTT transform; see Fig. 9e; and Contour; see Fig. 9f. Fig. 9a,b shows that the empirical probability-dots of the UHN model closely match the theoretical probability-line than others. The fitted UHN density line in Fig. 9b accurately captures the Shasta reservoir data histograms. The estimated reliability line of the UHN model (in Fig. 9c) matched the empirical reliability line compared to others. Fig. 9d also illustrates that the Shasta reservoir data set has an increasing failure rate. Ultimately, Fig. 9e indicates that the acquired MLE of σ existed and is unique. Henceforward, we suggest using $\sigma \equiv 3.7199$ as an initial guess for any additional calculations.

Now, from Table 13, three IAPT2C samples are created based on FP=50% and several choices of $\mathbf{R}$ and $T_i,\ i = 1, 2$; see Table 15. For each produced sample, the offered point and interval estimators developed via LF, SF, Bayes-LF, and Bayes-SF are calculated. In Table 16, the point estimates (along their SErrs) as well as the 95% interval estimates (along their interval widths (IWs)) of σ, $R(t)$, and $h(t)$ (at $t = 0.35$) are reported. By employing improper gamma priors, we assess the obtained Bayes and HPD interval estimators through the MCMC sampler, executing 30,000 iterations and discarding the first 5000 results. For evaluation logic, we set $a = b = 0.001$ in the proposed density prior.

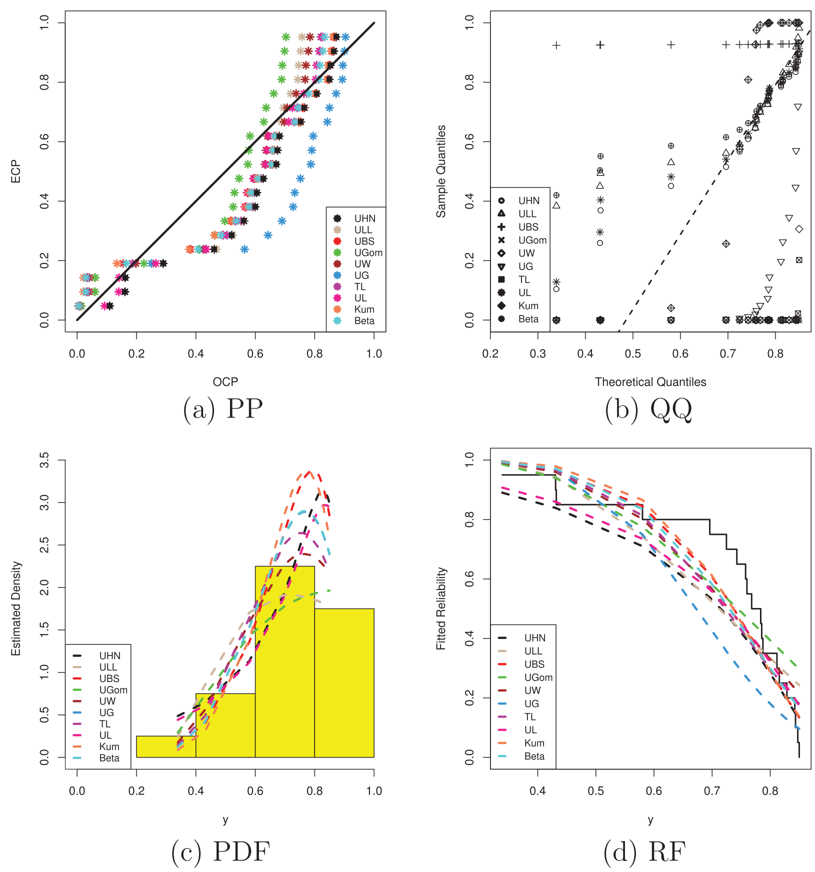

(a) PP (b) QQ (c) PDF (d) RF

Figure 9: (Continued)

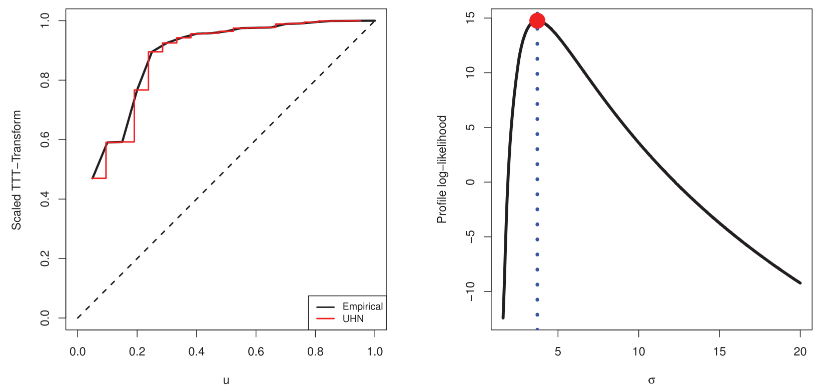

(e) TTT (f) Contour

Figure 9: Fitting visualizations of the UHN and its competitors from Shasta reservoir data

Table 15: Artificial IAPT2C samples from Shasta reservoir data

Sample	**R**	$T_1(d_1)$	$T_2(d_2)$	R^*	T^*	Data
S [1]	$(5, 5, 0^8)$	0.40(1)	0.79(10)	5	0.787408	0.338936, 0.431915, 0.580194, 0.724626, 0.757583, 0.759932, 0.768007, 0.783660, 0.785339, 0.787408
S [2]	$(0^4, 5, 5, 0^4)$	0.70(5)	0.79(9)	6	0.79	0.338936, 0.430681, 0.431915, 0.580194, 0.695970, 0.742563, 0.759932, 0.768007, 0.785339
S [3]	$(0^8, 5, 5)$	0.76(9)	0.80(10)	5	0.785339	0.338936, 0.430681, 0.431915, 0.580194, 0.695970, 0.724626, 0.742563, 0.757583, 0.759932, 0.785339

Table 16 states that the offered frequentist point (or interval) estimates of σ, $R(t)$, or $h(t)$ developed via the likelihood (spacings) approach behave similarly to each other, while their performance is less than that developed via the Bayes-LS (Bayes-SF) approach in terms of their SErrs and IWs.

Table 16: Estimates of σ, $R(t)$, and $h(t)$ from Shasta reservoir data

Sample	Par.	MLE MPSE		Bayes-LF Bayes-SF		95% ACI-LF 95% ACI-SF			95% HPD-LF 95% HPD-SF		
		Est.	SErr	Est.	SErr	Lower	Upper	IW	Lower	Upper	IW
S [1]	σ	4.5489	1.1160	4.3315	0.2619	2.3616	6.7363	4.3747	4.0369	4.5919	0.5549
		4.7617	1.1111	4.5397	0.2668	2.5840	6.9395	4.3554	4.2400	4.8168	0.5767
	$R(0.1)$	0.9805	0.0048	0.9795	0.0012	0.9711	0.9899	0.0187	0.9780	0.9807	0.0027
		0.9814	0.0043	0.9805	0.0011	0.9729	0.9899	0.0170	0.9793	0.9818	0.0025
	$h(0.1)$	0.2208	0.0552	0.2324	0.0141	0.1126	0.3290	0.2164	0.2187	0.2494	0.0307
		0.2107	0.0501	0.2215	0.0130	0.1126	0.3089	0.1963	0.2064	0.2350	0.0286
S [2]	σ	5.5775	1.5236	5.3549	0.2674	2.5912	8.5637	5.9725	5.0557	5.6328	0.5771
		5.8294	1.5189	5.6069	0.2674	2.8523	8.8065	5.9541	5.3077	5.8848	0.5771
	$R(0.1)$	0.9841	0.0043	0.9834	0.0008	0.9756	0.9926	0.0170	0.9826	0.9844	0.0018
		0.9848	0.0040	0.9842	0.0007	0.9770	0.9926	0.0155	0.9834	0.9850	0.0016
	$h(0.1)$	0.1794	0.0498	0.1872	0.0094	0.0818	0.2770	0.1952	0.1762	0.1967	0.0205
		0.1716	0.0454	0.1786	0.0085	0.0826	0.2605	0.1779	0.1686	0.1873	0.0187
S [3]	σ	5.3278	1.3710	5.1055	0.2672	2.6407	8.0149	5.3742	4.8060	5.3831	0.5771

(Continued)

Table 16 (continued)

Sample	Par.	MLE MPSE		Bayes-LF Bayes-SF		95% ACI-LF 95% ACI-SF			95% HPD-LF 95% HPD-SF		
		Est.	SErr	Est.	SErr	Lower	Upper	IW	Lower	Upper	IW
		5.5513	1.2505	5.3289	0.2673	3.1003	8.0022	4.9019	5.0296	5.6066	0.5771
	$R(0.1)$	0.9834	0.0043	0.9826	0.0009	0.9750	0.9918	0.0168	0.9817	0.9837	0.0020
		0.9840	0.0036	0.9834	0.0008	0.9770	0.9911	0.0141	0.9825	0.9843	0.0018
	$h(0.1)$	0.1880	0.0492	0.1965	0.0103	0.0916	0.2843	0.1927	0.1845	0.2070	0.0226
		0.1803	0.0413	0.1881	0.0094	0.0994	0.2611	0.1617	0.1771	0.1978	0.0207

To show that the acquired frequentist estimates of σ exist and are unique, for samples S[i] for $i = 1, 2, 3$, both profile-log-LF and profile-log-SF diagrams are shown in Fig. 10. It demonstrates, for each sample created from Shasta reservoir, that the MLE (or MPSE) of σ existed and is unique.

To check the convergence of MCMC iterations produced from LF (or SF), from Sample S [1] (as an example), Fig. 11 illustrates the density and trace plots of σ, $R(t)$, and $h(t)$. In each MCMC plot, the solid and dashed lines represent the Bayes and HPD interval estimates, respectively. All diagrams in Fig. 11 exhibit that the convergence of MCMC-LF (or MCMC-SF) iterations occurs well. They also support the same results as shown in Table 16. Additionally, the fitted Gaussian kernels from MCMC-LF (or MCMC-SF) iterations in Fig. 11 indicate that the iterations of σ are high symmetrical while those of $R(t)$ and $h(t)$ are near to negatively and positively skewed, respectively.

To sum up, the estimated parameter σ reflects variability in the transformed February water levels of the Shasta reservoir, capturing natural hydrological fluctuations, measurement uncertainty, and unobserved influences during 1991–2010.

7 Optimal PT2C

In reliability trials, the practitioner in charge wants to choose the best way to stop the trial from a bunch of options. Therefore, choosing the most effective ways to censor data has received a lot of attention in statistical research. For instance, you can refer to the work of Ng et al. [39], Pradhan and Kundu [40], Elshahhat and Abu El Azm [41], and Elshahhat et al. [42], as well as other researchers. Finding the best way to collect samples involves figuring out the method that gives us the most information about the unknown factors. In Table 17, we use different ways to select the best PT2C plan.

It is important to mention that the various criteria in Table 17 are evaluated at the MLE (or MPSE) of the unknown parameter σ. Regarding $\mathcal{M}_1$, after collecting an IAPT2C sample, we aim to maximize the estimated Fisher information acquired from the LF (or SF). Further, regarding $\mathcal{M}_2$, we aim to minimize the trace of the inverted Fisher information obtained from the same frequentist approaches. Moreover, $\mathcal{M}_3$ serves to reduce the variance of the log-MLE (or log-MPSE) of the qth quantile, such as

$$\log(\Sigma_q) = \log\left\{\frac{\sigma\Phi^{-1}(0.5(q+1))}{1+\sigma\Phi^{-1}(0.5(q+1))}\right\},\ 0 < q < 1,$$

where $\Phi^{-1}(\cdot)$ denotes the standard normal percentile and the variance of $\log(\Sigma_y)$ is approximated using the delta method. To pick the optimum PT2C scenario, one should select the censoring that gives the highest value of $\mathcal{M}_1$ and the lowest values of the other metrics.

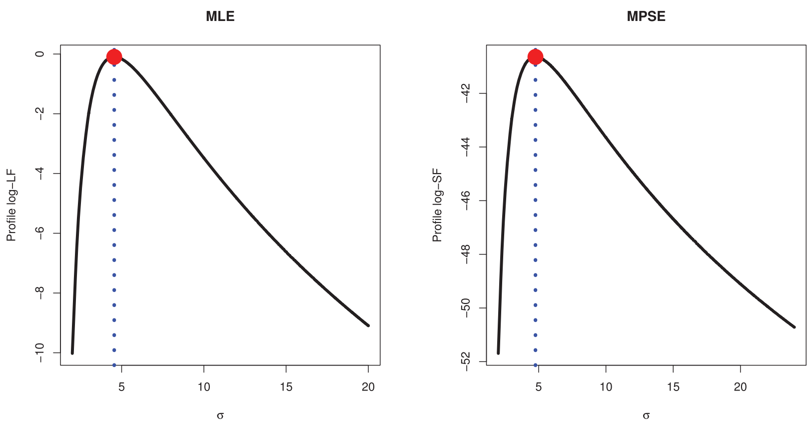

(a) Sample S[1]

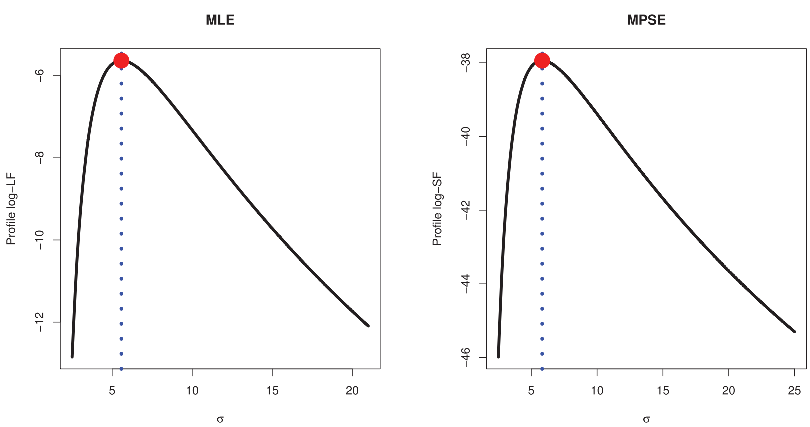

(b) Sample S[2]

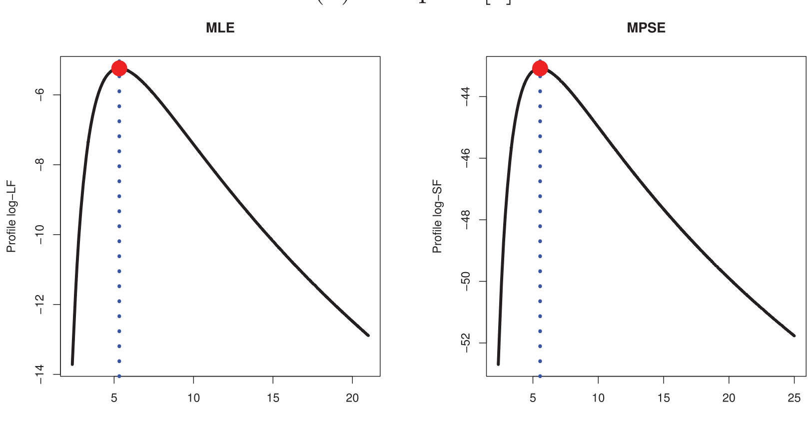

(c) Sample S[3]

Figure 10: Profiles for log-LF (left) and log-SF (right) of γ from Shasta reservoir data

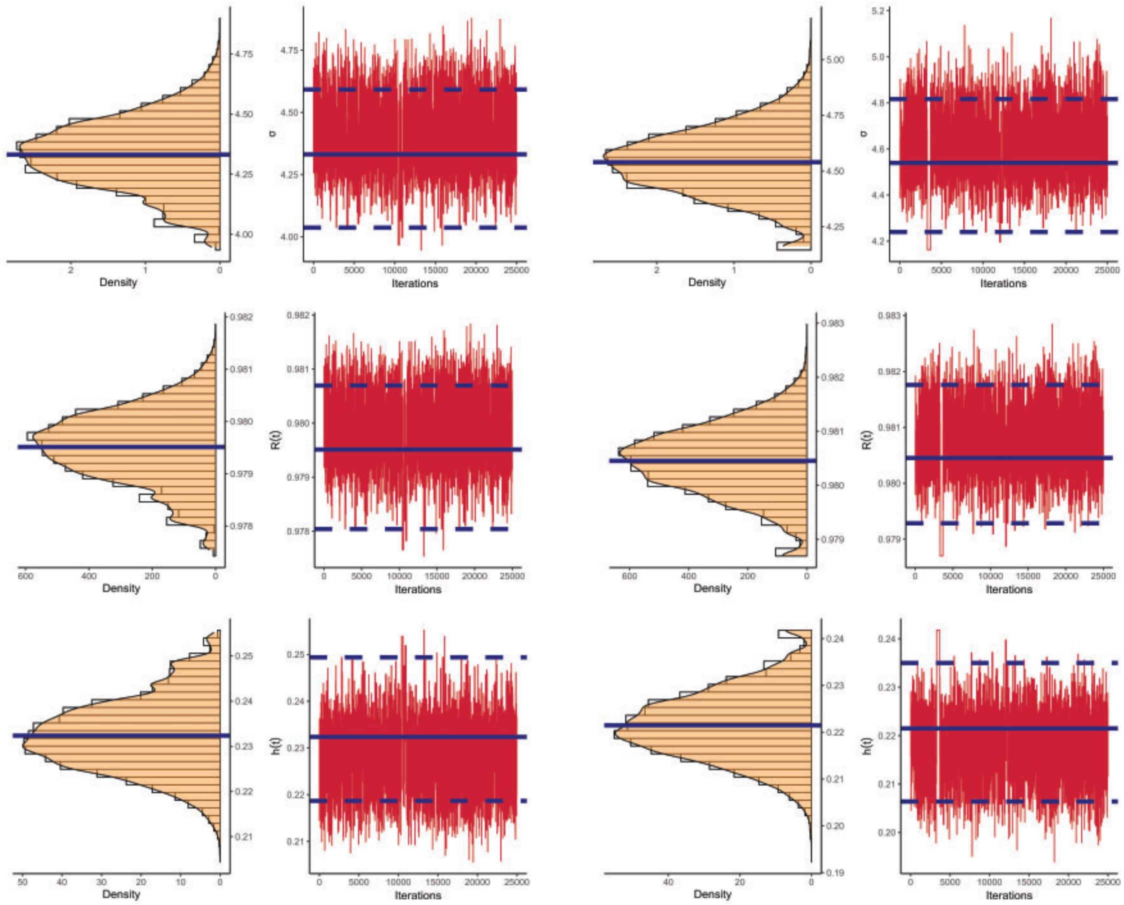

(a) MCMC-LF (b) MCMC-SF

Figure 11: Plots for 25,000 MCMC-LF and MCMC-SF iterations of σ, $R(t)$, and $h(t)$ from Shasta reservoir data

Table 17: Optimal PT2C metrics

Criterion	Description
$\mathcal{M}_1$	Maximize $\rightarrow -\dfrac{\mathrm{d}}{\mathrm{d}\sigma^2}L(\sigma\,\vert\,\underline{\mathbf{y}})$
$\mathcal{M}_2$	Minimize $\rightarrow \left[-\dfrac{\mathrm{d}}{\mathrm{d}\sigma^2}L(\sigma\,\vert\,\underline{\mathbf{y}})\right]^{-1}$
$\mathcal{M}_3$	Minimize $\rightarrow \widehat{var}(\log(\Sigma_q)),\ 0 < q < 1$

Now, to find the best PT2C from Shasta reservoir data, all metrics reported in Table 17 are evaluated through the offered frequentist estimates displayed in Table 16; see Table 18. According to likelihood (or spacing) results, Table 16 shows that the PT2C plan used in S [1] is the best based on $\mathcal{M}_i,\ i = 1, 2$, while the PT2C plan used in S [3] is the best based on $\mathcal{M}_3$ compared to others. It is best to remember here that the idealized PT2C scenario developed from the Shasta Reservoir data supports the oversight recommended in Section 5.

Table 18: Optimum PT2C scenario from Shasta reservoir data

Sample	$\mathcal{M}_1$	$\mathcal{M}_2$	$\mathcal{M}_3$		
$q \rightarrow$			0.3	0.6	0.9
Likelihood Method					
S [1]	0.80291	1.24546	0.00322	0.00162	0.00065
S [2]	0.43077	2.32144	0.00350	0.00156	0.00059
S [3]	0.53202	1.87963	0.00321	0.00147	0.00056
Spacings Method					
S [1]	0.81002	1.23454	0.00284	0.00139	0.00055
S [2]	0.43343	2.30717	0.00308	0.00134	0.00050
S [3]	0.63949	1.56375	0.00239	0.00107	0.00040

8 Concluding Remarks

In this study, we have introduced a range of estimation techniques for the unit half-normal distribution, presenting it as a novel and effective tool for reliability analysis using improved adaptive progressive Type-II censoring samples. By estimating the scale parameter, reliability function, and hazard rate function, the model demonstrates flexibility and offers a better fit compared to several existing models. The estimation issues addressed include both point and interval estimations for the scale parameter and reliability measures. Our comparative evaluation of classical and Bayesian methods demonstrates the model's precision in estimating critical metrics, such as reservoir reliability and hazard rates, while simulations and the Shasta Reservoir case study validate its practical utility. Moreover, some criteria are proposed for selecting the optimal progressive censoring plan, which is applied to the Shasta reservoir data. The results provide actionable insights for water resource policymakers, particularly in optimizing dam safety protocols and adaptive reservoir management. Beyond hydrology, the model's bounded nature and computational efficiency position it as a promising tool for ecological applications, such as wetland capacity estimation or rainfall infiltration modeling. Future work will prioritize refining policy-relevant outputs (e.g., risk thresholds for infrastructure failure) and extending the framework to other bounded systems, such as pollutant dispersal or soil moisture retention. These directions aim to bridge statistical techniques with tangible environmental decision-making, fostering resilience in resource management. An important direction for future research is the application of censored regression models in the context of improved adaptive progressive censoring data.

Acknowledgement: The authors would like to express thank to the Editor-in-Chief and anonymous referees for their constructive comments and suggestions. The authors extend their appreciation to the Deanship of Scientific Research and Libraries in Princess Nourah bint Abdulrahman University for funding this research work through the Research Group project, Grant No. (RG-1445-0024).

Funding Statement: The authors extend their appreciation to the Deanship of Scientific Research and Libraries in Princess Nourah bint Abdulrahman University for funding this research work through the Research Group project, Grant No. (RG-1445-0024).

Author Contributions: The authors confirm contribution to the paper as follows: study conception and design: Ohud A. Alqasem, Mazen Nassar; data collection: Maysaa Elmahi Abd Elwahab; analysis and interpretation of results: Ahmed Elshahhat; draft manuscript preparation: Mazen Nassar, Ahmed Elshahhat. All authors reviewed the results and approved the final version of the manuscript.

Availability of Data and Materials: The data that support the findings of this study are available within the paper.

Ethics Approval: Not applicable.

Conflicts of Interest: The authors declare no conflicts of interest to report regarding the present study.

References

1. Bakouch HS, Nik AS, Asgharzadeh A, Salinas HS. A flexible probability model for proportion data: unit-half-normal distribution. Communicat Statist: Case Stud Data Anal Applicat. 2021;7(2):271–88. doi:10.1080/23737484.2021.1882355.
2. Akdoğan Y, Ozkan E, Karakaya K, Tanış C. Estimation of parameter for inverse Rayleigh distribution under Type-I hybrid censored samples. Sigma J Eng Nat Sci. 2020;38(4):1705–11.
3. Balakrishnan N, Kannan N, Lin CT, Wu SJS. Inference for the extreme value distribution under progressive Type-II censoring. J Stat Comput Simul. 2004;74(1):25–45. doi:10.1080/0094965031000105881.
4. Rastogi MK, Tripathi YM. Estimating the parameters of a Burr distribution under progressive type II censoring. Stat Methodol. 2012;9(3):381–91. doi:10.1016/j.stamet.2011.10.002.
5. Dey S, Elshahhat A, Nassar M. Analysis of progressive type-II censored gamma distribution. Comput Stat. 2023;38(1):481–508. doi:10.1007/s00180-022-01239-y.
6. Anakha KK, Chacko VM. Statistical estimation of exponential power distribution on different progressive Type-II censoring schemes. J Indian Soc Probab Stat. 2024;25(1):85–120. doi:10.1007/s41096-023-00172-7.
7. Ng HKT, Kundu D, Chan PS. Statistical analysis of exponential lifetimes under an adaptive Type-II progressive censoring scheme. Naval Res Logist. 2009;56(8):687–98. doi:10.1002/nav.20371.
8. Ye ZS, Chan PS, Xie M, Ng HKT. Statistical inference for the extreme value distribution under adaptive Type-II progressive censoring schemes. J Stat Comput Simul. 2014;84(5):1099–1114. doi:10.1080/00949655.2012.740481.
9. Hemmati F, Khorram E. On adaptive progressively Type-II censored competing risks data. Communicat Statist-Simulat Computation 2017;46(6):4671–93. doi:10.1080/03610918.2015.1129408.
10. Nassar M, Abo-Kasem OE. Estimation of the inverse Weibull parameters under adaptive type-II progressive hybrid censoring scheme. J Computat Appl Mathem. 2017;315(12):228–39. doi:10.1016/j.cam.2016.11.012.
11. Kumari R, Sultana F, Tripathi YM, Sinha RK. Parametric inference for inverted exponentiated family with jointly adaptive progressive type-II censoring. Life Cycle Reliab Safety Eng. 2025;14(1):37–56. doi:10.1007/s41872-024-00281-7.
12. Lv Q, Tian Y, Gui W. Statistical inference for Gompertz distribution under adaptive type-II progressive hybrid censoring. J Appl Stat. 2024;51(3):451–80. doi:10.1080/02664763.2022.2136147.
13. Yan W, Li P, Yu Y. Statistical inference for the reliability of Burr-XII distribution under improved adaptive Type-II progressive censoring. Appl Mathem Modell. 2021;95:38–52. doi:10.1016/j.apm.2021.01.050.

14. Asadi S, Panahi H, Anwar S, Lone SA. Reliability estimation of burr type III distribution under improved adaptive progressive censoring with application to surface coating. Eksploatacja I Niezawodność. 2023;25(2):163054. doi:10.17531/ein/163054.
15. Dutta S, Kayal S. Inference of a competing risks model with partially observed failure causes under improved adaptive type-II progressive censoring. Proc Institut Mechan Eng Part O: J Risk Reliab. 2023;237(4):765–80. doi:10.1177/1748006x221104555.
16. Alam FMA, Nassar M. On entropy estimation of inverse Weibull distribution under improved adaptive progressively type-II censoring with applications. Axioms. 2023;12(8):751. doi:10.3390/axioms12080751.
17. Zhang L, Yan R. Parameter estimation of Chen distribution under improved adaptive type-II progressive censoring. J Stat Comput Simul. 2024;94(13):2830–61. doi:10.1080/00949655.2024.2358828.
18. Alotaibi R, Nassar M, Elshahhat A. Analysis of reliability indicators for inverted lomax model via improved adaptive type-II progressive censoring plan with applications. Complexity. 2024;2024(1):4848673. doi:10.1155/2024/4848673.
19. Cheng RCH, Amin NAK. Estimating parameters in continuous univariate distributions with a shifted origin. J R Stat Soc B. 1983;45(3):394–403. doi:10.1111/j.2517-6161.1983.tb01268.x.
20. Ranneby B. The maximum spacing method. An estimation method related to the maximum likelihood method. Scand J Stat. 1984;11(2):93–112.
21. Ozkan E, Simsek GC, Tanış C. Maximum product spacing estimation for odd lindley half logistic distribution under progressive type-II censoring with binomial removals. Int J Ind Eng: Theor Appl Pract. 2024;31(6):1382–91. doi:10.23055/ijietap.2024.31.6.10133.
22. Innocent CF, Frederick OA, Udofia EM, Obulezi OJ, Igbokwe CP. Estimation of the parameters of the power size biased Chris-Jerry distribution. Int J Innovat Sci Res Technol. 2023;8(5):423–36.
23. Alsadat N, Hassan AS, Elgarhy M, Chesneau C, Mohamed RE. An efficient stress—strength reliability estimate of the unit Gompertz distribution using ranked set sampling. Symmetry. 2023;15(5):1121. doi:10.3390/sym15051121.
24. Abonongo AIL, Abonongo J. Exponentiated generalized weibull exponential distribution: properties, estimation and applications. Computat J Mathem Statist Sci. 2024;3(1):57–84. doi:10.21608/cjmss.2023.243845.1023.
25. Dutta S, Dey S, Kayal S. Bayesian survival analysis of logistic exponential distribution for adaptive progressive Type-II censored data. Comput Stat. 2024;39(4):2109–55. doi:10.1007/s00180-023-01376-y.
26. Henningsen A, Toomet O. maxLik: a package for maximum likelihood estimation in R. Comput Stat. 2011;26(3):443–58. doi:10.1007/s00180-010-0217-1.
27. Plummer M, Best N, Cowles K, Vines K. CODA: convergence diagnosis and output analysis for MCMC. R News. 2006;6:7–11.
28. Nassar M, Elshahhat A. Estimation procedures and optimal censoring schemes for an improved adaptive progressively Type-II censored Weibull distribution. J Appl Stat. 2023;51(9):1664–88. doi:10.1080/02664763.2023.2230536.
29. Nadar M, Papadopoulos A, Kızılaslan F. Statistical analysis for Kumaraswamy's distribution based on record data. Stat Pap. 2013;54(2):355–69. doi:10.1007/s00362-012-0432-7.
30. Korkmaz MÇ, Korkmaz ZS. The unit log-log distribution: a new unit distribution with alternative quantile regression modeling and educational measurements applications. J Appl Stat. 2023;50(4):889–908. doi:10.1080/02664763.2021.2001442.
31. Mazucheli J, Menezes AF, Dey S. The unit-Birnbaum-Saunders distribution with applications. Chilean J Statist. 2018;9(1):47–57.
32. Mazucheli J, Menezes AF, Dey S. Unit-Gompertz distribution with applications. Statistica. 2019;79(1): 25–43.

33. Mazucheli J, Menezes AFB, Fernandes LB, De Oliveira RP, Ghitany ME. The unit-Weibull distribution as an alternative to the Kumaraswamy distribution for the modeling of quantiles conditional on covariates. J Appl Stat. 2020;47(6):954–74. doi:10.1080/02664763.2019.1657813.
34. Mazucheli J, Menezes AFB, Dey S. Improved maximum-likelihood estimators for the parameters of the unit-gamma distribution. Commun Stat—Theory Methods. 2018;47(15):3767–78. doi:10.1080/03610926.2017.1361993.
35. Topp CW, Leone FC. A family of J-shaped frequency functions. J Am Stat Assoc. 1955;50(269):209–19. doi:10.1080/01621459.1955.10501259.
36. Mazucheli J, Menezes AFB, Chakraborty S. On the one parameter unit-Lindley distribution and its associated regression model for proportion data. J Appl Stat. 2019;46(4):700–14. doi:10.1080/02664763.2018.1511774.
37. Mitnik PA, Baek S. The Kumaraswamy distribution: median-dispersion re-parameterizations for regression modeling and simulation-based estimation. Stat Pap. 2013;54(1):177–92. doi:10.1007/s00362-011-0417-y.
38. Gupta AK, Nadarajah S. Handbook of beta distribution and its applications. Boca Raton, FL, USA: CRC press; 2004.
39. Ng HKT, Chan PS, Balakrishnan N. Optimal progressive censoring plans for the Weibull distribution. Technometrics. 2004;46(4):470–81. doi:10.1198/004017004000000482.
40. Pradhan B, Kundu D. On progressively censored generalized exponential distribution. Test. 2009;18(3):497–515. doi:10.1007/s11749-008-0110-1.
41. Elshahhat A, Abu El Azm WS. Statistical reliability analysis of electronic devices using generalized progressively hybrid censoring plan. Qual Reliab Eng Int. 2022;38(2):1112–30. doi:10.1002/qre.3058.
42. Elshahhat A, Dutta S, Abo-Kasem OE, Mohammed HS. Statistical analysis of the Gompertz-Makeham model using adaptive progressively hybrid Type-II censoring and its applications in various sciences. J Radiat Res Appl Sci. 2023;16(4):100644. doi:10.1016/j.jrras.2023.100644.